University of South Bohemia in České Budějovice
Faculty of Science

Design and production of TBEV specific cleavage reporter for in vitro and in cell studies

Master thesis

Bc. Eliška Kotounová, BSc

Supervisor: RNDr. Zdeněk Franta, Ph.D.

Co-supervisor: Mgr. Tomáš Fessl, Ph.D.

České Budějovice 2021

Kotounová, E., 2021: Design and production of TBEV specific cleavage reporter for in vitro and in cell studies. Mgr. Thesis, in English. – 66 p., Faculty of Science, University of South Bohemia, České Budějovice, Czech Republic.

Annotation:

Tick-borne encephalitis virus (TBEV) is an important human pathogen and as of now, there are no specific therapeutics to combat this disease. *In vitro* and in cell models are essential in studying the disease and in the pursuit of novel therapeutics. This thesis deals with the design and production of two genetically encoded cleavage reporters of TBEV NS2B-NS3 protease activity. The reporters were produced in *E. coli* and tested with recombinant NS2B-NS3 protease, as well as produced in mammalian cell lines and analyzed for fluorescence upon infection with TBEV.

Declaration:

I declare that I am the author of this qualification thesis and that in writing it I have used the sources and literature displayed in the list of used sources only.

České Budějovice, 13.12.2021

.....

Bc. Eliška Kotounová, BSc.

Acknowledgments:

First and foremost, I would like to express my gratitude to my supervisor RNDr. Zdeněk Franta, Ph.D. for his guidance and valuable advice that he has provided me with throughout the whole time in the lab. My thanks also belong to my co-supervisor Mgr. Tomáš Fessl, Ph.D. for his supervision of the fluorescence experiments but also for his patience as I came to this part of the work with little to no previous experience.

This work would not be possible without the kind provision of TBEV by Mgr. Zuzana Beránková, and the recombinant TBEV NS2B-NS3 protease by Paulina Duhita Anindita, Ph.D..

I would also like to thank to the whole team of the Makrokomplex lab, especially to my dear colleagues and friends Mgr. Barbora Kaščáková and Mgr. Petra Havlíčková, for their help and support in both professional and personal spheres.

Table of contents

List of abbreviations

ADE – antibody-dependent enhancement

AIDS – acquired immune deficiency syndrome

APS – ammonium persulfate

ATP – adenosine triphosphate

BBB – blood-brain barrier

BHK – baby hamster kidney cells

BOFES – bovine fetal serum

bp – base pair

C – capsid protein

CNS – central nervous system

CV – column volume

ddH_2O – double-distilled water

DENV – dengue viruses

DENV-2 – dengue virus, serotype 2

DMEM – Dulbecco's modified eagle medium

dNTP – deoxynucleoside triphosphate

E – envelope protein

EDTA – ethylenediaminetetraacetic acid

ER – endoplasmic reticulum

FB – Fluorobrite DMEM

hMGFP – Monster Green® Fluorescent Protein

hpi – hours post-infection

hpt – hours post-transfection

HS – heparan sulfate

IMAC – immobilized metal affinity chromatography

IPTG – isopropyl β-D-1-thiogalactopyranoside

JEV – Japanese encephalitis virus

kb – kilobase

kDa – kilodalton

LB – lysogeny broth

LBP – laminin-binding protein

LGTV – Langat virus

M – membrane protein

MM – master mix

MOI – multiplicity of infection

MS – mass spectrometry

MTase – methyltransferase

NC – nucleocapsid

NKV – no known vector virus

NS – non-structural protein

NS2B-NS3pro – NS2B-NS3 protease

OD_{600} – optical density measured at 600 nm

OHFV – Omsk haemorrhagic fever virus

PAGE – polyacrylamide gel electrophoresis

PAmCherry – photoactivatable mCherry

PBS – phosphate-buffered saline

PCR – polymerase chain reaction

PDB – protein databank

PFU – plaque-forming unit

prM – precursor membrane protein

QP – quenching peptide

RC – replication complex

RdRp – RNA-dependent RNA polymerase

rpm – revolutions per minute

rSAP – shrimp alkaline phosphatase

RT-PCR – real-time PCR

SBR – signal-to-background ratio

SDS – sodium dodecyl sulfate

SOC – super optimal broth with catabolite repression

SP – structural protein

spp – several species (two or more)

ssRNA – single-stranded RNA

TAE – Tris-acetate-EDTA

TBE – tick-borne encephalitis

TBEV – tick-borne encephalitis virus

TBS – Tris-buffered saline

TE – Tris-EDTA

TEMED – tetramethylethylenediamine

UTR – untranslated region

UV – ultraviolet

WNV – West Nile virus

YFV – yellow fever virus

ZIKV – Zika virus

1 Introduction

1.1 *Flaviviridae*

Family *Flaviviridae* is classified among the positive single-stranded RNA (+ssRNA) viruses and its representatives are causative agents of various human diseases such as encephalitis, haemorrhagic disease, jaundice, biphasic fever, or flaccid paralysis [1]. The majority of these viruses are arthropod-borne viruses (arboviruses), which are transmitted by mosquitoes or ticks. Mosquito-borne viruses represent yellow fever virus (YFV) (transmitted by *Aedes* spp), dengue viruses (DENV) (*Aedes aegypti*), Japanese encephalitis virus (JEV) (*Culex* spp), West Nile virus (WNV) (*Culex* spp), and Zika virus (ZIKV) (*Aedes* spp), while tick-borne flaviviruses include tick-borne encephalitis virus (TBEV) (*Ixodes* spp) and Omsk haemorrhagic fever virus (OHFV) (*Ixodes* and *Dermacentor* spp) [1, 2]. However, there exist flaviviruses whose transmission cycles are restricted to only arthropod or vertebrate hosts. These are referred to as no known vector flaviviruses (NKV) [3].

The epidemiology of flaviviruses widely depends on the ecological demand of the vertebrate hosts and the invertebrate vectors. The spread of the arboviruses can be minimized by the prevention of the contact between the host and the vector; however, due to the involvement of many hosts and vectors, control of these viruses remains challenging. In addition, an increase in temperatures, traveling, and transport results in the spread of the arboviruses into new areas, thus increasing the incidence of infections [1]. There are effective vaccines to combat YFV, DENV, JEV, and TBEV, but there are none approved against WVN and ZIKV [2]. Moreover, no specific therapy is available for patients suffering from any flaviviral disease; hence, it is important to study the conserved features of the flavivirus life cycle in search for potential targets of new broad-spectrum antivirals [4].

1.2 Tick-borne encephalitis virus (TBEV)

TBEV is the most important human tick-borne pathogen in Europe and north-eastern Asia, which infects the central nervous system (CNS). Although the majority of infections are asymptomatic, symptomatic infections cause meningitis, encephalitis, and meningoencephalitis. These manifestations are collectively called tick-borne encephalitis (TBE). In its severe form, TBE can lead to life-long neurological problems or death [5, 6]. The mortality rate of TBEV depends on the particular subtype, with the major three subtypes

being the European (TBEV-Eu), Siberian (TBEV-Sib), and Far Eastern (TBEV-FE) [7]. European subtype is predominant across Europe, partly in Russia and the infections are generally mild with a mortality rate of < 2%. The other two subtypes can be found primarily in Asia. While Siberian subtype infections are generally mild with a tendency to cause chronic infections and a low mortality rate (2-3%) [8], the Far Eastern subtype causes the most severe TBE with a significantly increased mortality rate up to 40% [6].

1.2.1 Tick-borne encephalitis virus: transmission

TBEV is transmitted by ticks of family *Ixodidae*, namely *Ixodes ricinus* in Europe and *Ixodes persulcatus* in Asia [5]. Nonetheless, TBEV can be transmitted as a food-borne upon consumption of unpasteurized dairy milk and milk products contaminated by TBEV [9].

TBEV cycles between ticks and mammalian hosts. Rodents serve as TBEV reservoir, as well as maintenance hosts because they can keep persistent infection during the year. Ticks get infected by TBEV during feeding on an infected host. Upon TBEV infection, the tick remains infected for the rest of its life and can further pass the virus to various vertebrate hosts or uninfected ticks during co-feeding. In addition, the transovarial transmission of TBEV has been reported [10].

Ixodes ricinus has a three-host life cycle undergoing four life stages – an egg, a larva, a nymph, and an adult, which feed on a host from a range of species. After feeding on the host, the tick detaches and molts in leaves (larva, nymph) or lays a clutch of eggs and dies (adult female) [10, 11]. The life-cycle is shown in Figure 1.

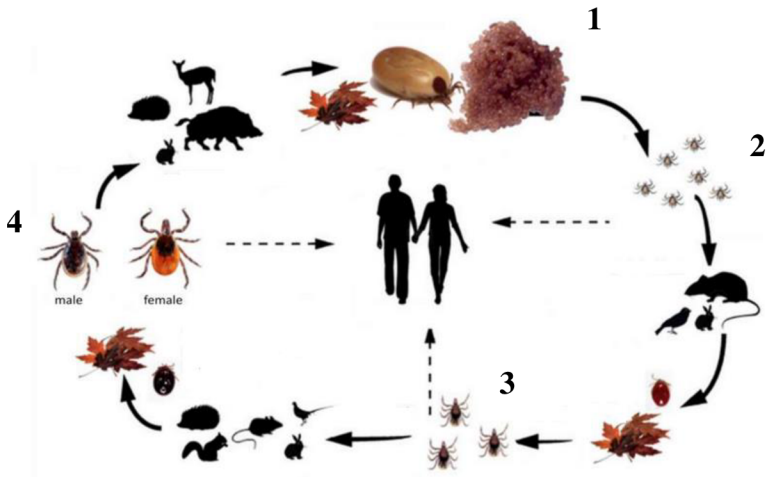

Figure 1 – **Schematic representation of *Ixodes ricinus* life-cycle.** From laid egg (1) a larva (2) hatches and feeds on a host. After detaching from the host, it molts in leaves to nymph (3), which feeds on a new host. Nymphs molt into adult ticks (4). The adult female feeds on the new host and lays a clutch of eggs and dies. Potential transmission of TBEV to humans is shown by dotted arrows, in the case of adults, only females can transmit the virus [11].

1.2.2 Tick-borne encephalitis virus: pathogenesis

TBEV virions enter the host body during tick feeding together with tick saliva, which components have been shown to enhance TBEV transmission [12]. At the onset of infection, the virus replicates locally in Langerhans cells and neutrophils of the skin and is transported by migrating monocytes and macrophages into the draining lymph nodes, where it replicates further and spreads to the bloodstream, causing primary viremia [13]. Presence of viral particles in blood results in infection of peripheral organs and tissues, leading to secondary viremia. The virus then crosses the blood-brain barrier (BBB), which triggers brain infection. There are several proposed mechanisms of how TBEV crosses BBB, however, the exact mechanism remains enigmatic and it is likely the combination of various mechanisms [14]. The infection is often cleared by the immune system at the stage of primary viremia. The immune response includes the interferon responses, action of natural killer and antigen-presenting cells, antibody-mediated humoral response, and the cell-mediated response, as reviewed by Ruzek et al. (2019) [5].

The incubation period of TBE is between 7 and 14 days (can range from 2 to 28 days) and has two phases. The first phase consists of viremia, which causes fever, headache, fatigue, nausea, or vomiting. Monophasic TBE ends after this phase and the virus does not enter the CNS. During the second phase (so-called biphasic TBE) virus penetrates into CNS and neurological symptoms manifest. TBEV also has the ability to persist in the CNS, causing ongoing infection, and leading to chronic TBE. The first phase of TBE can be identified from blood via real-time PCR (RT-PCR), while the second phase is diagnosed using serological tests. The biphasic TBE is observed in approximately one-third of the patients [5].

1.2.3 Tick-borne encephalitis virus: morphology

TBEV is a smooth, icosahedral enveloped virus with a diameter of 50 nm. It consists of a nucleocapsid and host-derived lipid bilayer with embedded membrane (M) and envelope proteins (E). The nucleocapsid (NC) is built of 60 capsid dimers (C) and one copy of the viral genome. The viral genome is approximately 11 kb long +ssRNA, encoding a single polyprotein, which is processed to three structural and seven non-structural proteins [5, 6, 15]. A schematic of the virus particle is shown in Figure 2.

The characteristic symmetry of the particle is provided by heterodimers of E and M proteins that coat the lipid envelope, as the NC does not follow the icosahedral symmetry [16].

Protein E composes the majority of the TBEV particle and it has several functions such as interaction with the host receptors [17], the exit of the virus from the cells [18], or a role in the virus neurovirulence [19]. Fusogenic property of E protein is crucial for entry of TBEV NC into cytoplasm as the protein mediates fusion of the viral and host membranes [18]. M protein is much smaller and as it is completely hidden in the interface of the E-E homodimer, it was suggested that it has a role in keeping and strengthening the interaction between the molecules of E protein. It is also responsible for the maturation of the viral particles, in a process where the precursor of M protein (prM) is cleaved to M protein [15].

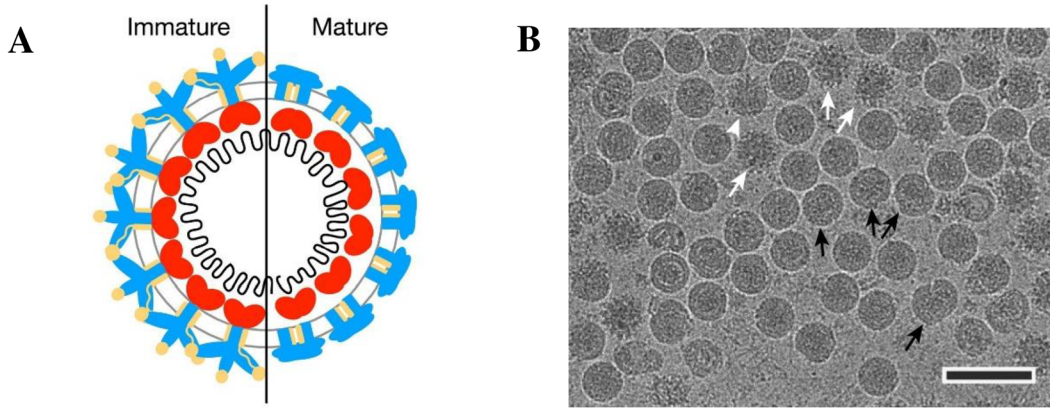

Figure 2 – **TBEV virion.** A – Schematic representation of mature and immature TBEV virion. Yellow – prM protein, blue – E protein, red – capsid dimers, black – viral RNA [20]. B – Cryo-EM image of mature, immature (white arrow), half-mature (white arrowhead), and damaged (black arrow) TBEV particles. Scale bar represents 100 nm [15].

1.2.4 Tick-borne encephalitis virus: replication cycle

The replication cycle is well described for many mosquito-borne flaviviruses, however for TBEV much less information is available. The process is complex and requires several maturation steps to produce infectious particles as shown in Figure 3 [6]. TBEV enters the cells via receptor-mediated endocytosis. The primary interaction is mediated by receptors on the host cell and the TBEV surface glycoprotein E. Laminin-binding protein (LBP) [21], αVβ3 [22], and glycosaminoglycan heparan sulfate (HS) [23] have been identified as potential receptor candidates in mammalian cells. A recent study by Rodriguez et al. (2019) [24] conducted with Langat virus (LGTV), which is naturally attenuated representative of TBEV complex with high amino acid identity, showed that the virus-host interaction might be dependent on the cellular type and involve more than a single host cell receptor. In addition, it has been shown that TBEV, like other flaviviruses, undergoes a phenomenon called antibody-dependent enhancement (ADE), where the infectivity is increased upon the presence of a specific antibody [25].

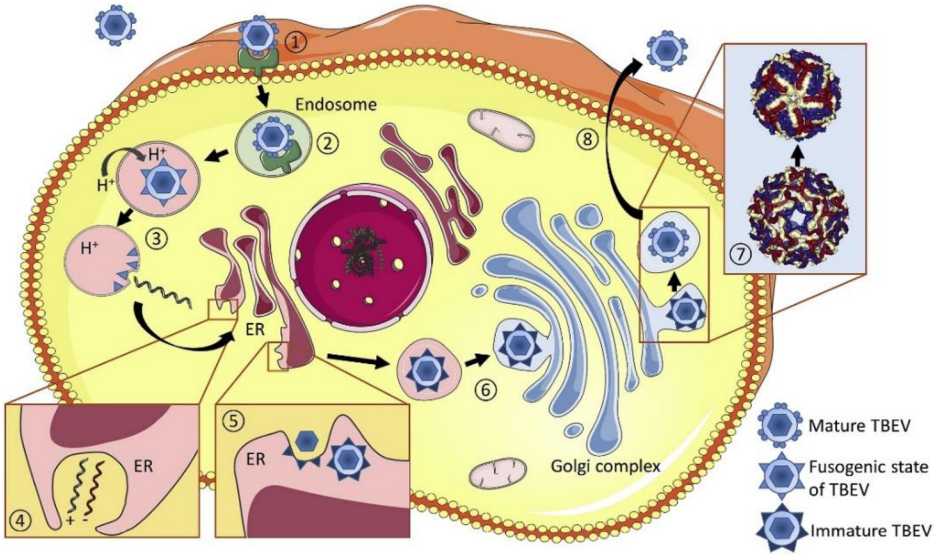

Figure 3 – **Schematic representation of TBEV replication cycle.** 1 – binding of TBEV to a receptor, 2 – endocytosis of viral particles, 3 – virion uncoating, 4 – replication in invaginations of endoplasmic reticulum (ER), 5 – virus assembly in the lumen of ER, 6 – transport of immature particles to Golgi apparatus, 7 – maturation of viral particles, 8 – virus release [5].

The receptor-mediated endocytosis results in the transport of viral particles into endocytic compartments, where structural changes of glycoprotein E from dimers to trimers are induced by low pH that leads to the fusion of the endocytic membrane with the viral membrane [26]. Membrane fusion causes a release of the NC into the cytoplasm of the host cell. Viral RNA is then uncoated and translated on the ribosomes of the endoplasmic reticulum (ER) as a single polyprotein (Figure 4). This polyprotein is subsequently cleaved by both viral and host enzymes into three structural proteins (SP) and seven non-structural proteins (NS). While the SPs form the virion, NS proteins take part in the genome replication, processing of the polyprotein, and modulation of cell functions [6]. Summary of all proteins and their proposed functions are given in Table 1.

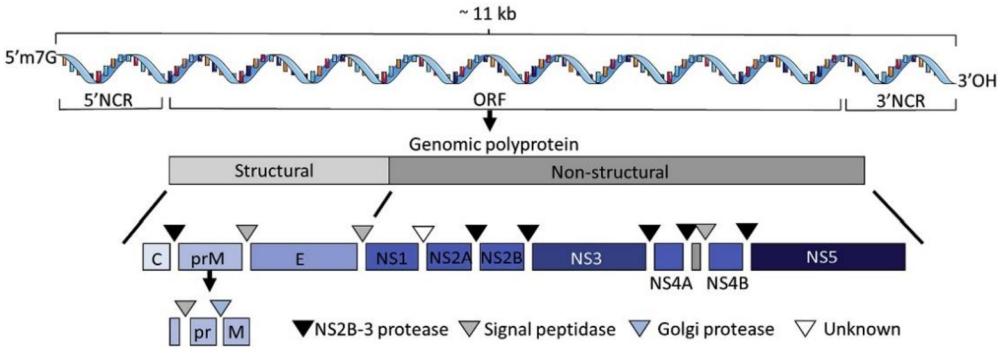

Figure 4 – **Flaviviral polyprotein and its processing into structural and non-structural proteins** [5].

Table 1 – **TBEV proteins and their functions as reviewed by Pulkinnen et al. (2018)** [6].

Protein	Localization in cell	Function
capsid protein (C)	cytoplasm (after cleavage of membrane anchor)	RNA binding, formation of nucleocapsid, immunomodulation
envelope protein (E)	lumen of ER	cellular attachment, membrane fusion, antibody target
membrane protein (M)	lumen of ER	the surface structure of the virion
NS1	lumen of ER	replication, immunomodulation
NS2A	integral membrane protein	particle assembly, replication, immunomodulation
NS2B	integral membrane protein	particle assembly, co-factor of NS3 protease
NS3	cytoplasm	protease/helicase activity
NS4A	integral membrane protein	regulation of ATP activity of NS3
NS4B	integral membrane protein	replication complex formation, immunomodulation
NS5	cytoplasm	RNA-dependent RNA polymerase (RdRp), methyltransferase (MTase)

TBEV replicates on the membrane of ER where viral NS proteins and host factors interact and form a so-called replication complex (RC). New genomes are synthesized inside RC and captured by C protein to form nucleocapsids on the cytoplasmic side of ER. This interaction is mediated by electrostatic interactions between the highly positively charged residues on α4 helix and viral RNA [27] and without any sequence specificity as shown for C protein of ZIKV and DENV [28, 29]. However, it has been suggested that the NS2A protein interacts with the 3' UTR of the viral RNA and recruits it to the site of assembly [30, 31].

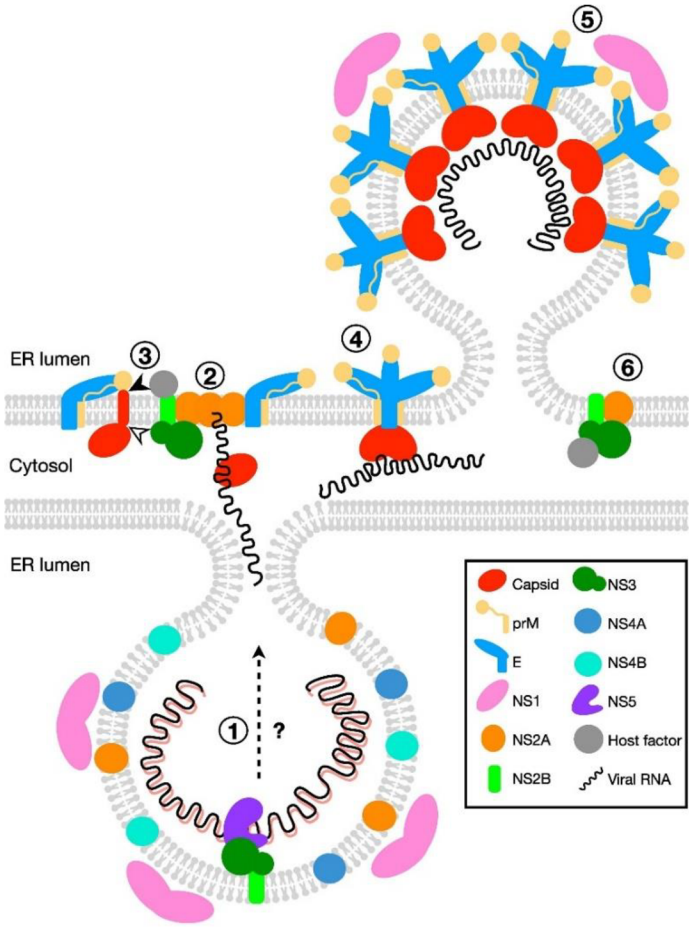

Figure 5 – **Schematic representation of replication complex and virion assembly.** 1 – transfer of synthesized RNA from RC to NS2A, 2 – association of RNA with NS2A, prM-E complexes and NS2B-NS3, 3 – host signalase and NS2B-NS3 protease cleave capsid-prM junctions, allowing for association with RNA, 4 – formation of assembly unit of the virion from capsid dimers and prM-E trimers, 5 – budding process stabilized NS1 protein, 6 – release of the immature virion into ER lumen by host endosomal sorting complexes [20].

After the assembly, the NC buds into the ER where it obtains the lipid envelope and structural proteins E and prM. Generally, three types of viral particles are produced during transport from ER through Golgi apparatus: immature non-infectious, partially mature, and mature infectious. EM structure of TBEV immature particles has been described by Füzik et al. (2018) [15] and is shown in Figure 2 (see 1.2.3). Immature particles contain prM protein, which has not yet been cleaved and thus the surface of the particle comprises of heterodimers of prM and E organized into trimeric spikes [32]. The immature virions released from ER go through the Golgi apparatus to the trans-Golgi compartment, where the low pH leads to a conformational change in the prM-E trimer spikes, and maturation is finished by cleavage of pr peptide from prM by host cell furin protease. The cleavage of pr peptide gives virion the ability to fuse with membranes, thus making it infectious. This maturation process is often incomplete so immature and partially mature particles can be released from

the infected cell. Immature particles are non-infectious due to a lack of ability to fuse with membranes, while partially mature particles can infect new host cells [6].

1.3 NS2B-NS3 protease (NS2B-NS3pro)

NS3 is a highly conserved polyfunctional protein possessing both helicase and protease activity [33]. It is the second-largest flaviviral protein with a size of 69 kDa. The N-terminal domain of NS3 is the chymotrypsin-like protease, which has a role in the processing of TBEV polypeptide into individual proteins, while the C-terminal domain of NS3 acts as NTPase-dependent RNA helicase [34]. For its proper function, the NS3 protease domain requires an NS2B protein as a cofactor. NS2B is a smaller protein of 14 kDa possessing two transmembrane regions on its N- and C-terminus. These two hydrophobic transmembrane segments anchoring NS2B into ER membrane are connected by a hydrophilic loop of 47 amino acids, which acts as the cofactor of the NS3 protease domain [35, 36]. NS2B cofactor regulates NS3 proteolytic activity by stabilizing the correct protein fold as well as participation on substrate cleavage site [37].

The flaviviral NS2B-NS3pro is specifically responsible for the cleavage of the capsid protein from its membrane anchor to generate mature capsid protein, as well as for cleavage on the N-terminus of NS2B, NS3, NS4A, and NS5 [33]. The active site of the protease consists of catalytic triad typical for serine proteases – histidine (51), aspartic acid (75), and serine (135). The protease recognizes and cleaves after two basic residues (arginine or lysine) at the P1 and P2 positions. The key residues for substrate recognition, which explain the structure-activity relationship, have been identified in the work of Erbel et. al (2006) [38] by crystallographic studies of NS3 protease from DENV and WNV with inhibitors. The S1 pocket is formed by glycine, tyrosine, threonine, and aspartic acid residues, with an aspartic acid residue located at the bottom of the pocket, which similarly as in trypsin molecule stabilizes the positive charge of the substrate residue. The S2 pocket is predominantly formed by negative electrostatic potential from oxygen atoms of the backbone of the NS2B cofactor, which again stabilize the positive charge of the substrate molecule. These findings explain the importance of basic residues in positions P1 and P2. Currently, there is no structure yet for the TBEV NS2B-NS3 protease, however, crystal structures are available for proteases from DENV [39, 38], WNV [35], and ZIKV [40]. Crystal structures of DENV NS2B-NS3 protease and WNV NSB2-NS3 protease in the presence of inhibitor are shown in Figure 6.

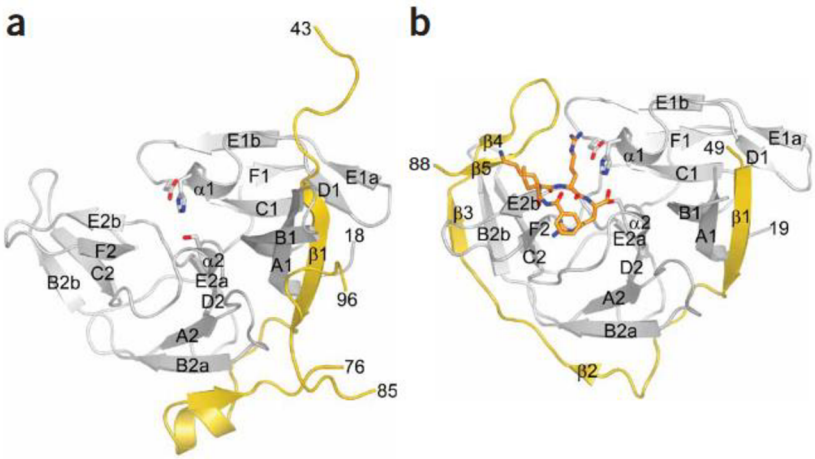

Figure 6 – **Crystal structure NS2B-NS3 protease.** a – DENV NS2B-NS3 protease without inhibitor, NS2B shown in yellow, NS3 protease in grey (PDB ID: 2FOM). b – WNV NS2B-NS3 in the presence of inhibitor Bz-Nle-Lys-Arg-Arg-H (orange) (PDB ID: 2FP7) [38].

1.3.1 Targeting NS2B-NS3 protease for drug development

As shown by Chambers et al. (1993) [41], the NS2B-NS3pro is crucial for the replication of flaviviruses. The mutants of YFV carrying the inactive NS2B-NS3pro failed to produce infectious viral particles upon infection of baby hamster kidney (BHK) cells. Therefore, viral proteases present a suitable target for drug development. As of now, several viral protease inhibitors have been approved as drugs in the treatment of AIDS such as ritonavir, amprenavir, or lopinavir [42], or hepatitis C such as telaprevir, simeprevir, or grazoprevir [43].

Numerous mutagenesis studies have been performed with both NS2B and NS3, as reviewed by Li et al. (2017) [43], showing that mutation of the residues in the active site or its close surrounding resulted in complete or almost complete loss of function. Mutations further from the active site led to a medium reduction of the protease activity. In addition, some mutations in NS2B-NS3pro were shown to be correlated with viral pathogenicity. In the work of Potapova et. al (2012) [44], mutations in the TBEV NS3 protein 16 R→K and 45 S→F were investigated for their effect on the TBEV NS2B-NS3pro complex conformation by molecular dynamics simulations. Highly pathogenic strains contain 16 R and 45 S residues, and the substitution for 16 K and 45 F in poorly pathogenic strains results in the local shift in the protease hydrophobicity, which leads to the global change of the protease conformation. These mutations causing differences in protease structure could be useful for the development of TBEV drugs.

Initial inhibition studies on DENV-2 NS2B-NS3pro by Leung et al. (2001) [45] showed that standard serine protease inhibitors do not inhibit the protease complex, except for aprotinin. A further study reported that aprotinin inhibits all four DENV serotypes with high affinity making it a potent flavivirus NS2B-NS3pro inhibitor [46], however, aprotinin also binds trypsin and other serine proteases in the body. It was used as a blood loss prevention agent in complex surgeries until the drug was withdrawn from the market due to the increased risk of complications or death [47, 48]. Additionally, peptidic α-keto amide inhibitors [45], protein inhibitors [49], or small-molecule inhibitors [50–53] were investigated for their inhibition towards NS2B-NS3pro. Yet these inhibitors, in general, showed rather low inhibition in cell-based assays or presented other problems such as poor bioavailability, poor penetration, or poor stability. All these inhibitors were targeted for the active site of the protease, which might be the reason for limited success with this approach as the active site of the flavivirus protease is flat and highly charged [39, 38, 35], which limits the potential for small-molecule inhibitors. Another possible target for inhibition presents the association site between the NS2B cofactor and NS3 protease. Based on the structure of the NS2B-NS3pro complex [35, 38, 39] a small-molecule inhibitor of NS2B-NS3 interaction was identified [54], which shows that allosteric inhibition of this interaction can be a valid therapeutic target.

Although many inhibitors of viral proteases have been described so far, there has been only a little information about inhibitors of TBEV NS2B-NS3pro. First and as of now the only reported inhibitors of TBEV protease come from the work of Akaberi et al. (2021) [55]. The TBEV protease complex was modeled based on the available crystal structures of the complex from other flaviviruses (ZIKV, DENV, and WNV). A tripeptide Compound 86, which shows inhibitory activity against ZIKV, WNV, and DENV proteases, was tested *in silico* and also with recombinant TBEV protease in *in vitro* assays. Compound 86, as well as Compound 104 and 6C, which differ only by different basic residues in P1 and P2 positions, exhibited promising inhibitory activity against TBEV NS2B-NS3pro and provide a good starting point for further design of inhibitors for TBEV NS2B-NS3pro. The binding poses of Compound 86 with the TBEV protease are shown in Figure 7.

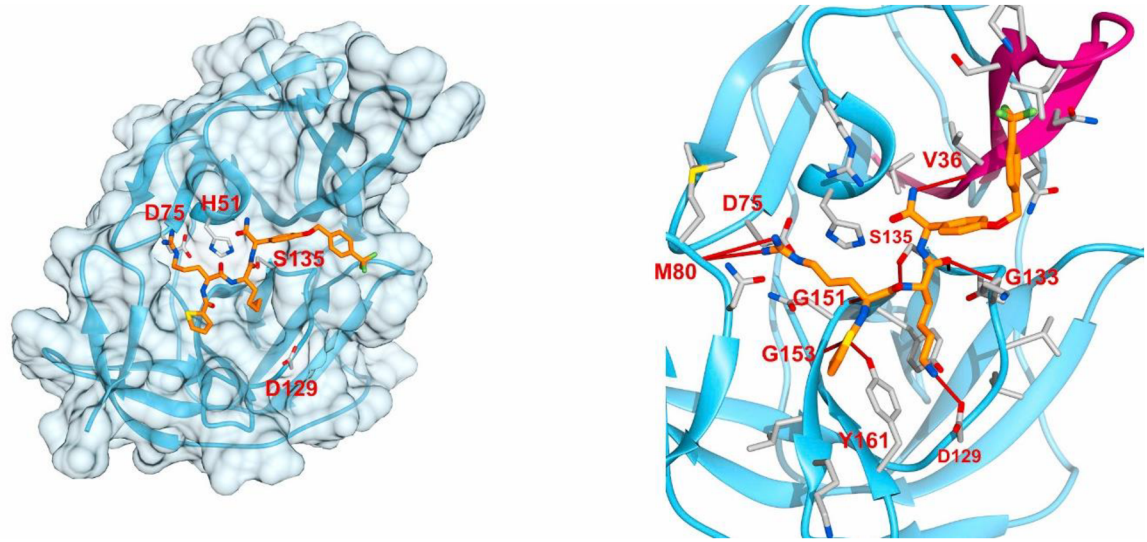

Figure 7 – **Modelling of binding of Compound 86 and TBEV protease showing results from molecular docking (left) and molecular dynamic simulations' cluster analysis (right).** Catalytic triad, negatively charged aspartate residues in the S1 and S2 pocket are shown as sticks [55].

The design of antiviral drugs requires a good understanding of virus-host interaction kinetics. Current approaches for monitoring of viral infection in living cells mostly rely either on immunostaining [56], use of recombinant viruses [57], viral replicons [58–60], or molecular reporters of NS2B-NS3pro activity [61, 62]. However, these methods present limitations for in cell studies or are not suitable for studies of native virus strains or clinical isolates. Better approaches to study and monitor virus infection in living cells could provide valuable insight into the mechanisms of the infection and offer a tool for analysis of putative inhibitors in cell-based assays. A recent study by Arias-Arias et al. (2020) [63] reports the construction of a genetically based fluorescent molecular reporter of NS2B-NS3pro activity in DENV, ZIKV, and YFV. The flavivirus-activatable reporter was built of a fluorescent protein, specific protease cleavage site, and quenching peptide, which prevents maturation of the fluorescent protein, and therefore the fluorescence signal is detected only upon cleavage of the quenching peptide off the reporter by the NS2B-NS3pro. The quenching peptide alters the oligomeric state of the protein, leading to the formation of higher state oligomers thus preventing the chromophore formation and keeping the fluorescent protein in the dark state [64]. Based on this work, we have developed a fluorescent reporter for TBEV NS2B-NS3pro using two different fluorescent proteins – photoactivatable mCherry (PAmCherry) and Monster Green® Fluorescent Protein (hMGFP).

2 Goals

In this thesis, the following goals were set:

1. design and cloning of recombinant cleavage reporter into various vectors

2. production and purification of recombinant cleavage reporter using *E. coli* expression system

3. establishment of mammalian stable cell lines expressing cleavage reporter

3 Material and methods

3.1 Solutions and buffers

Table 2 – **Composition of used solutions in order of appearance in the text.**

Name	Composition
50X TAE	242 g Tris, 57.1 mL acetic acid, and 100 mL 0.5M EDTA in 1 L dH_2O
1X TAE	dilution of 50X TAE in 1 L dH_2O
general lysis buffer	50mM KH_2PO_4, 400mM NaCl, 100mM KCl, 10% glycerol, 0.5% TritonX-100, 10mM imidazole, pH = 7.8
4X Laemmli buffer	20mL of 0.5M Tris (pH = 6.8), 4g SDS, 20 mL glycerol, 0.1 g of bromphenol blue, dH_2O up to 45mL
4X SDS-PAGE sample buffer	900 µL of 4X Laemmli buffer and 100 µL β-mercaptoethanol
1X SDS-PAGE buffer	dilution of 4X SDS-PAGE sample buffer in 1X PBS
10X SDS-PAGE running buffer	250 mM Tris, 1.92 M glycine, 1% SDS
1X SDS-PAGE running buffer	dilution of 10X SDS-PAGE running buffer in 1L dH_2O
fixing solution	50% ethanol, 2% phosphoric acid
staining solution	1.2 g Coomassie Blue G-250, 23.4 mL phosphoric acid, 100 g $(NH_4)_2SO_4$, dH_2O up to 800 mL, 200 mL 100% methanol
10X SDS-PAGE transfer buffer	58.15g Tris, 29.3g glycine, 3.75g SDS in 1L dH_2O
1X SDS-PAGE transfer buffer	dilution of 10X SDS-PAGE transfer buffer into 900 mL dH_2O, addition of 100 mL methanol
10X TBS buffer	60.5g Tris, 87.66g NaCl in 1L dH_2O, pH = 7.6
1X TBS-T	dilution of 10X TBS buffer into 1L, addition of 1 mL Tween20
purification lysis buffer	20 mM Tris, 100 mM NaCl, pH = 7.5 + protease inhibitor + DNase I
solubilization buffer	6M guanidium hydrochloride, 50 mM Tris, pH = 7.5
PAmCherry rep - equilibration buffer denaturing	6M urea, 100 mM NaCl, 20 mM Tris, pH = 8
PAmCherry rep - elution buffer denaturing	6M urea, 100 mM NaCl, 20 mM Tris, 0.5M imidazole, pH = 8
PAmCherry rep - refolding buffer A	4 M urea, 100 mM NaCl, 20 mM Tris, 20 mM β-mercaptoethanol, pH = 8
PAmCherry rep - refolding buffer B	100 mM NaCl, 20 mM Tris, 1 mM β-mercaptoethanol, pH = 8

PAmCherry rep - refolding buffer C	100 mM NaCl, 20 mM Tris, pH = 8
hMGFP rep - equilibration buffer native	100 mM NaCl, 20 mM Tris, pH = 8.5
hMGFP rep - elution buffer native	100 mM NaCl, 20 mM Tris, 0.5M imidazole, pH = 8.5
hMGFP rep - equilibration buffer denaturing	6M urea, 100 mM NaCl, 20 mM Tris, pH = 8.5
hMGFP rep - elution buffer denaturing	6M urea, 100 mM NaCl, 20 mM Tris, 0.5M imidazole, pH = 8.5
hMGFP rep - refolding buffer A	4 M urea, 100 mM NaCl, 20 mM Tris, 20 mM β-mercaptoethanol, pH = 8.5
hMGFP rep - refolding buffer B	100 mM NaCl, 20 mM Tris, 1 mM β-mercaptoethanol, pH = 8.5
hMGFP rep - refolding buffer C	100 mM NaCl, 20 mM Tris, pH = 8.5

3.2 Construct design

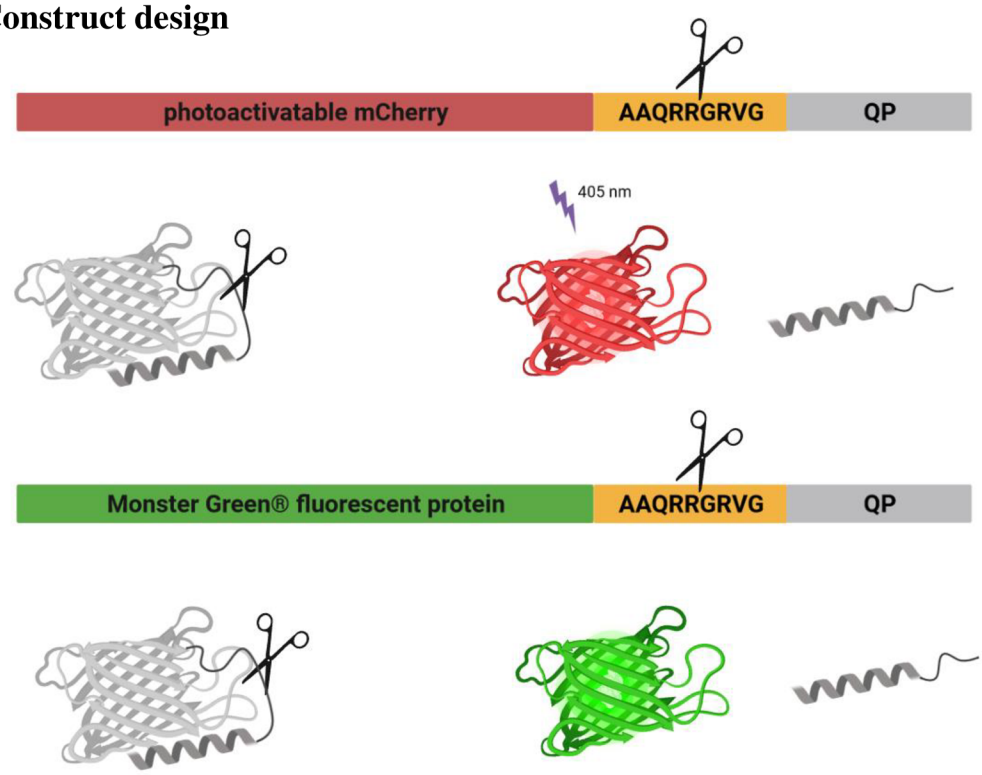

Figure 8 – **Schematic representation of both constructs.** Each construct consists of the fluorescent protein, TBEV NS2B-NS3 protease cleavage site, and quenching peptide (QP) (created with biorender.com).

Both constructs, PAmCherry_reporter, and hMGFP_reporter were assembled using Gibbson assembly into pUC19 cloning vector and recloned into the desired expression plasmid. Each construct contained the fluorescent protein (either PAmCherry or hMGFP) on the N-terminus, followed by TBEV NS2B-NS3 protease cleavage site and C-terminal inhibition peptide derived from the transmembrane domain of influenza M2 protein (Figure 8). Gene-specific primers suitable for individual cloning step have been designed either manually or using NEBuilder Assembly Tool (http://nebuilder.neb.com/#!/) and are listed in Table 3.

Table 3 – **Specific primers used for amplification of the fragments.**

Primer	Sequence	Cloning vector	Restriction enzyme
pPAmCherry_linker_R	AGAGGATCCCCGGGTACCGATTAAAGACGATCAAGAATCCACAATATCAAGTGCAAGATCCCAATGATACTCGCAGCAACAACAAGCGGGTCACTTGAATCGTTGCAACCAACTCTTCCGCGCCGTTGGGCAGC*CTTGTACAGCTCGTCCATGC*	pUC19	-
pPAmCherry_F	GACGGCCAGTGAATTCGAGC*ATGGTGAGCAAGGGCGAG*	pUC19	-
pPAmCherry_rep_CR_NdeI_F	ATGGTA**CATATG***GTGAGCAAGGGCGAG*	pET21b, pET19b	NdeI
pPAmCherry_rep_CR_XhoI_R	ATGGTA**CTCGAG***AAGACGATCAAGAATCCACAATATCAAGTG*	pET21b	XhoI
pPAmCherry_rep_CR_STOP_R	ATGGTA**CTCGAG***TTAAAGACGATCAAGAATCCACAATATCAAGTG*	pET19b	XhoI
pPAmCherry_rep_attB_F	GGGGACAAGTTTGTACAAAAAAGCAGGCTTCGAAGGAGATAGAACC*ATGGTGAGCAAGGGCGAG*	pDONR207	-
pPAmCherry_rep_attB_R	GGGGACCACTTTGTACAAGAAAGCTGGGTTTTA*AAGACGATCAAGAATCCACAATATCAAGTG*	pDONR207	-
pUC19_inhib_F	*GCTGCCCAACGGCGCGGA*	pUC19	-
pUC19_inhib_R	*GCTCGAATTCACTGGCCGTCGTTTTACAACG*	pUC19	-
hMGFP_F	GACGGCCAGTGAATTCGAGC*ATGGGCGTGATCAAGCCCGACATG*	pUC19	-
hMGFP_R	CTTCCGCGCCGTTGGGCAGC*GCCGGCCTGGCGGGGTAG*	pUC19	-
hMGFP_rep_F	ATGGTA**CATATG***GGCGTGATCAAGCCCGA*	pET21b	NdeI
hMGFP_rep_attB_F	GGGGACAAGTTTGTACAAAAAAGCAGGCTTCGAAGGAGATAGAACC*ATGGGCGTGATCAAGCCCGACATG*	pDONR207	-
hMGFP_control_R	ATGGTA**CTCGAG***GCCGGCCTGGCGGGG*	pET21b	XhoI

Note: (1) The restriction site for each enzyme is highlighted in bold and underlined.

(2) The gene-specific part in each primer is shown in cursive.

(3) The first primer contains the TBEV NS2B-NS3 protease cleavage site and inhibition peptide sequence, these are marked in blue and red respectively.

3.3 Polymerase chain reaction (PCR)

3.3.1 Gradient PCR

All primers were tested for optimal annealing temperature by gradient PCR using PPP Master Mix (Top Bio), following the protocol from the manufacturer. The reactions were performed in Biometra TOne Thermal Cycler (Analytik Jena), with the setting of initial denaturation at 94°C for 1 min followed by 30 cycles of 3 step repetition: (1) denaturation at 94°C for 15 sec, (2) primer annealing at given temperature range for 15 sec, (3) elongation at 72°C for 1 min/kb. The whole process was finished with the final extension at 72°C for 7 min, and the reaction mixture was then cooled down to 16°C. The composition of each reaction is given in Table 4. The template DNA was always diluted to final a concentration of 50-100 ng template per reaction.

Resulting amplicons were separated using 1% agarose gel (SERVA Electrophoresis), prepared in 1X TAE buffer, and stained with Serva DNA Stain Clear G (SERVA Electrophoresis). 100 bp DNA Ladder or 1 kb DNA Ladder (New England Biolabs) have been used with respect to expected amplicon size. Gels were run at 100 V for 45 min and visualized on G:BOX Chemi-XX6 (Syngene).

Table 4 – **Composition of reactions for gradient PCR.**

Reagent	Volume [µL]
PPP Master Mix	12.5
forward primer (10 µM)	2
reverse primer (10 µM)	2
ddH_2O	7.5
template DNA	1
total amount	25

3.3.2 PCR using Q5® High-Fidelity DNA Polymerase

For each cloning, the DNA fragment was amplified using Q5® High-Fidelity DNA Polymerase (New England Biolabs). The thermal cycler setting was based on the protocol from the manufacturer and consisted of initial denaturation at 98°C for 30 sec, followed by 35 cycles of denaturation at 98°C for 10 sec, primer annealing at a given temperature for 20 sec, and elongation at 72°C for 20 sec/kb. The final extension was done at 72°C for 2 min

and the reaction mixture was then kept at 16°C. Table 5 gives the composition of the reaction mixtures.

The samples were separated on 1% agarose gel as described above. Amplicons were cut out from the gel and the DNA was purified using NucleoSpin® Gel and PCR Clean-Up (Macherey-Nagel) according to the gel extraction protocol. DNA concentration was measured using NanoDrop One (Thermo Scientific).

Table 5 – **Composition of the reaction mixture for Q5® PCR amplification.**

Reagent	Volume [µL]
buffer (5X Q5 Reaction Buffer)	10
dNTPs (10 mM)	1
forward primer (10 µM)	2.5
reverse primer (10 µM)	2.5
Q5 High-Fidelity DNA Polymerase (2U/µL)	0.5
5X Q5 High GC Enhancer	10
template DNA	1
ddH_2O	22.5
total amount	50

3.4 NEBuilder® HiFi DNA Assembly

The assembly of individual constructs was done using NEBuilder® HiFi DNA Assembly (New England Biolabs) according to the manual instructions. Briefly, amplified gene products and pUC19 vector were mixed in the vector:insert ratio of 1:2. Next, HiFi Master Mix was added and the mixture was incubated for 30 min at 50°C, placed on ice, and transformed into NEB® 5-alpha Competent *E. coli* (New England Biolabs) according to recommended instructions. The exact amounts used in the individual reactions are shown in Table 6.

Table 6 – **Reaction mixtures composition for NEBuilder® HiFi DNA Assembly.**

Reagent	Amounts	Amounts
HiFi Master Mix	5 µL	5 µL
pUC19	0.04 pmol	0.04 pmol
PAmCherry	0.08 pmol	-
hMGFP	-	0.08 pmol
ddH2O	up to 10 µL	up to 10 µL

3.5 Restriction digestion

For cloning into pET21b and pET19b, restriction digestion was performed using NdeI and XhoI restriction enzymes. The DNA fragments and cloning vectors were mixed with buffer and respective enzymes and the reaction was incubated at 37°C for 15 min. The enzymes were deactivated at 65°C for 20 min. The exact composition of the reaction mixture is given in Table 7. Digested vectors were treated with 2.5 µL of shrimp alkaline phosphatase (rSAP) and incubated at 37°C for 30 min. rSAP was then inactivated at 65°C for 5 min. Digestion products were purified with NucleoSpin® Gel and PCR Clean-Up (Macherey-Nagel) following the PCR clean-up protocol.

Table 7 – **Composition of digestion reactions.**

Reagent	Amount
DNA - amplicon (PAmCherry_reporter or hMGFP_reporter)	1 µg
DNA – vector (pET21b or pET19b)	1 µg
10X CutSmart Buffer	5 µL
NdeI/XhoI	1 µL
ddH_2O	up to 50 µL

3.6 Ligation

Digested fragments and plasmids were mixed in a 3:1 (insert to vector) ratio and joined together by T4 DNA ligase (Invitrogen). Ligation was performed at 16°C overnight with a final inactivation step at 65°C for 10 min. Set up of the ligation reaction is presented in Table 8. 2 µL of ligation mixture was used for NEB® 5-alpha Competent *E. coli* (New England Biolabs) transformation.

Table 8 – **Ligation reactions set up.**

Reagent	Amount
10X T4 DNA ligase buffer	2 µL
T4 DNA ligase	1 µL
restricted plasmid (pET19b or pET21b)	0.02 pmol
PAmCherry_reporter or hMGPF_reporter	0.06 pmol
ddH_2O	up to 20 µL

3.7 Gateway cloning

Preparation of construct for expression of the protein in mammalian cells was done via the Gateway cloning system. The amplicon generated by PCR contained attB flanking sites

and it was inserted into pDONR207 vector using the Gateway™ BP Clonase™ II Enzyme mix (Invitrogen) according to the manufacturer's instructions. Briefly, the enzyme mix was mixed with equimolar amounts of DNA and incubated at 25°C overnight. Next day 1 μL of proteinaseK was added and the mixture was incubated at 37°C for 10 min. The exact composition of the reaction mixture is shown in Table 9. NEB® 5-alpha Competent *E. coli* (New England Biolabs) were transformed with 1 μL of the mixture as described in chapter 3.8 and incubated overnight at 37°C on LB-agar plates containing 10 μg/mL gentamicin. Obtained colonies were analyzed by colony PCR to confirm the presence of inserted gene as described in 3.9. Minipreps were prepared from positive colonies as specified in 3.10 and the incorporation of the target sequence was verified by sequencing.

Generated entry clones pDONR_PAmCherry and pDONR_hMGFP were used to transfer both reporters into pcDNA-pDEST40 expression vector using Gateway™ LR Clonase™ II Enzyme mix (Invitrogen) according to the instructions. Briefly, equimolar amounts of both plasmids were mixed with enzyme mix (Table 9). The reaction mixture was incubated at 25°C for 1 hour, then 1 μL of proteinaseK was added and the reaction mixture was incubated at 37°C for 10 min. Next 1 μL of the reaction mixture was added to NEB® 5-alpha Competent *E. coli* (New England Biolabs) and transformed as described in chapter 3.8 and incubated overnight at 37°C on LB-agar plates containing 100 μg/mL ampicillin. Colony PCR was used to confirm the presence of the gene of interest as described in 3.9. A positive colony was chosen and maxiprep was prepared as given in 3.10.

Table 9 – **Composition of BP and LR reactions.**

Reagent	BP reaction	LR reaction
BP Clonase™ II Enzyme mix	2 μL	-
LR Clonase™ II Enzyme mix	-	2 μL
TE buffer, pH = 8	up to 8 μL	up to 8 μL
PAmCherry_reporter or hMGFP_reporter	25 fmol	-
pDONR207	25 fmol	-
pDONR_PAmCherry or pDONR_hMGFP	-	20 fmol
pcDNA-pDEST40	-	20 fmol

3.8 Transformation of *E. coli* competent cells

Plasmids containing the gene of interest were transformed into various competent *E. coli* strains, either into NEB® 5-alpha (New England Biolabs) for the propagation of the plasmid or into BL21(DE3) (New England Biolabs), BL21-CodonPlus (Agilent

Technologies), One Shot® BL21(DE3)pLysS (Invitrogen), and Rosetta-gami® 2(DE3) (Novagen) cells for recombinant protein production. A vial of cells was thawed on ice for approximately 30 minutes and then a defined amount of reaction mixture/plasmid was added to the cells. The contents of the vial were gently mixed by finger flicking, and the vial was incubated on ice for 30 minutes, followed by heat shock in a water bath at 42°C for the time interval specified in Table 10. After heat shock, a vial with cells was placed on ice for 5 minutes and 250 µL of room temperature SOC medium (New England Biolabs) was added. Cells were incubated in an Eppendorf Innova® S44i horizontal shaker at 37°C, 220 rpm for 1 hour. Selection LB-agar plates containing appropriate antibiotics suitable for each plasmid and cell strain (as shown in Tables 10 and 11) were pre-warmed, cells were spread onto them and incubated overnight at 37°C.

Table 10 – **Heat shock length and antibiotic required for individual *E. coli* strain.**

Competent *E. coli* strain	Heatshock [s]	Required antibiotic	Final concentration [µg/mL]
NEB® 5-alpha	30	-	-
BL21(DE3)	10	-	-
BL21-CodonPlus	20	chloramphenicol	35
BL21(DE3)pLysS	30	chloramphenicol	35
Rosetta-gami 2(DE3)	30	chloramphenicol	35
		tetracycline	12.5

Table 11 – **Antibiotic resistances conferred to *E. coli* by individual plasmids.**

Plasmid	Antibiotic resistance	Final concentration [µg/mL]
pUC19	ampicillin	100
pET21b, pET19b	ampicillin	100
pDONR207	gentamicin	10
pcDNA-pDEST40	ampicillin	100

3.9 Colony PCR

Colonies obtained from *E. coli* transformation were verified for the presence of the gene of interest by colony PCR. Individual colonies were picked up with a pipette tip into 20 µL of ddH_2O and used as a DNA template for the reaction. From each colony, a cross on a pre-warmed LB plate was made and labeled numerically. PCR reaction was carried out according to the TopBio PPP Master Mix protocol (Table 4) and 1 µL of the colony template. The setting of the thermal cycler was in accordance with the setting described in 3.2.1, with

the addition of one extra step of the first denaturation step at 94°C for 6 min. Results of the reaction were visualized on 1% agarose gel to identify positive colonies.

3.10 Plasmid isolation and sequence verification

Positive colonies were placed into 3 mL of LB media supplied with given antibiotics according to Table 10 and 11 and incubated overnight in Eppendorf Innova® S44i horizontal shaker at 37°C and 220 rpm. Next day the cells were harvested by centrifugation at 11 000 x g for 1 min and plasmids were isolated with Nucleo-Spin® Plasmid kit (Macherey-Nagel) using High copy plasmid isolation protocol. Plasmid concentration was measured with NanoPhotometer® Pearl (Implen) and samples were sent for sequencing to SEQme company.

From each recombinant plasmid with a verified sequence, a maxiprep was prepared by inoculating cells from the colony PCR cross into 150 mL of LB media supplied with respective antibiotics. Cells were incubated overnight at 37°C and 180 rpm. The following day, the cells were harvested by centrifugation at 4 122 x g, 4°C for 10 min, and plasmids were isolated using Nucleobond® Xtra Midi kit (Macherey-Nagel) with High-copy plasmid purification protocol. Maxipreps from pcDNA-pDEST40 with both constructs were further purified by ethanol precipitation prior to transfection. The sample was mixed with 1/10 volume of 3M sodium acetate (Thermo Scientific) and 2 times the volume of 100% ethanol. The solution was incubated on ice for 15 min and placed in the freezer overnight. Next day the sample was centrifuged at 18 200 x g, 4°C for 30 min, the supernatant was discarded and 1 mL of 70% ethanol was added to wash the pellet. Then the sample was centrifuged again at 18 200 x g and 4°C for 15 min. The supernatant was discarded and the pellet was let to dry at room temperature until transparent. The purified plasmid was recovered in 200 uL of ddH_2O and concentration was measured with NanoDrop One (Thermo Scientific).

3.11 Pilot expression

Protein production in *E. coli* BL21(DE3), BL21-CodonPlus, BL21(DE3)pLysS, and Rosetta-gami 2(DE3) competent cells was evaluated by pilot expression experiment. A single colony of cells carrying the desired construct was added to 20 mL of LB media containing the respective antibiotics (Table 10 and 11). The culture was incubated overnight at 37°C and 220 rpm in an Eppendorf Innova® S44i horizontal shaker. The next day, an aliquot of 1 mL from the overnight culture was added into 15 mL of fresh LB media, supplemented with

corresponding antibiotics, and the culture was incubated at 37°C and 220 rpm until the OD_{600} of the culture reached 0.5-0.8. After reaching this value, the protein production was induced with 1 mM IPTG and cells were incubated in the shaker at 18°C or 30°C and 220 rpm. 1 mL sample was taken from each culture at specific time intervals, and cells were pelleted at 11 000 x g in a microcentrifuge for 1 min. The resulting cell pellets were stored at -20°C for further use.

3.12 SDS-PAGE

Cells harvested from pilot expression experiments were thawed at room temperature and resuspended in 0.5 mL of lysis buffer. Cell lysis was performed by 3 cycles of freezing in liquid nitrogen, followed by thawing at 42°C. Insoluble protein fraction was separated by centrifugation at 18 200 x g at 4°C for 5 min. The supernatant containing soluble protein fraction was removed from the pellet, transferred into a fresh tube, and mixed with 4X SDS-PAGE sample buffer. Samples were boiled for 5 min at 95°C. The insoluble protein pellet was mixed with 1X SDS-PAGE sample buffer and boiled for 5 min at 95°C.

Samples were analyzed on 10% or 12.5% SDS-PAGE gels, which were prepared according to Table 12. PageRuler™ Protein Prestained Ladder (Thermo Fischer Scientific) was added to each gel as molecular mass standard. SDS-PAGE was run at 100V for 1.5 hours in 1X SDS-PAGE running buffer. After the run, stacking gel was removed from the rest of the gel and the resolving gel was placed into 20 mL of fixing solution for 30 min. The gel was washed twice for 10 min in ddH_2O and stained with staining solution overnight. Gel images were taken using G:BOX Chemi-XX6 (Syngene).

Table 12 – **Composition of SDS-PAGE gels, amounts given for 1 gel.**

Reagent	Resolving gel (10%)	Resolving gel (12.5%)	Stacking gel (4%)
40% Acrylamide/Bis-acrylamide, 29:1 (Sigma-Aldrich)	1.25 mL	1.56 mL	0.25 mL
dH_2O	2.395 mL	2.08 mL	1.46 mL
1.5M Tris (pH = 8.8)	1.25 mL	1.25 mL	-
1M Tris (pH = 6.8)	-	-	0.25 mL
10% SDS	50 µL	50 µL	20 µL
10% APS	50 µL	50 µL	20 µL
TEMED	5 µL	5 µL	2 µL

3.13 Western blot

For the purpose of Western Blot, protein samples were separated via SDS-PAGE as described above. After the run, the gel was equilibrated in 1X SDS-PAGE transfer buffer on a rocking platform for 15 min. Meanwhile, an Immun-Blot® PVDF membrane (Biorad) was cut in the size of the gel and equilibrated in 100% methanol for 15 min followed by 15 min in 1X SDS-PAGE transfer buffer. The blotting sandwich was assembled from a pre-cut block of filter paper (13.5 cm x 8.6 cm) wetted with 1X SDS-PAGE transfer buffer, PVDF membrane, SDS-PAGE gel, and another stack of wetted filter paper block. The whole sandwich was pressed together using a roller to ensure no bubbles were present. The blotting sandwich was placed into a cassette of Trans-Blot® Turbo (Biorad) instrument and blotting run at 25V, 1A for 30 min. The membrane was removed from the blotting sandwich and washed 3x10 min in TBS-T on a rocking platform. Washed membrane was blocked in 5% Blotting-Grade Blocker Nonfat Dry Milk (Biorad) in TBS-T on a rocking platform for 1 hour at room temperature. The membrane was washed again 3x10 min in TBS-T on a rocking platform and incubated overnight at 4°C with mouse primary Monoclonal anti-polyhistidine antibody (Sigma, H1029) (1:3000) in 5% milk solution. Unbound antibodies were washed away by 3x10 min wash in TBS-T. Secondary goat Anti-mouse IgG-peroxidase antibody (Sigma, A5278) in dilution of 1:5000 in TBS-T was added to the membrane. The membrane was incubated on a rocking platform for 1 hour at room temperature and then washed 2x10 min in TBS-T and 1x10 min in TBS. Finally, the signal was developed using Clarity® Western ECL Substrate (Biorad) by mixing the components in a 1:1 ratio followed by incubation at room temperature for 5 min. The membrane was imaged with G:BOX Chemi-XX6 (Syngene).

3.14 Large scale protein production

Based on the analysis of pilot expression experiments, both recombinant proteins were produced on a large scale in pET21b in BL21-CodonPlus cells. PAmCherry reporter was produced at 30°C for 6 hours, while hMGFP reporter was produced at 18°C for 24 hours. Prior to large-scale expression, 20 mL overnight cultures supplied with 100 µg/mL ampicillin and 35 µg/mL chloramphenicol were prepared and incubated overnight at 37°C and 220 rpm. Overnight cultures were transferred to 800 mL of fresh LB media and incubated in an Eppendorf Innova® S44i horizontal shaker at 37°C and 220 rpm until the OD_{600} reached 0.5-0.8. Protein production was induced with 1mM IPTG and cells were incubated at 220 rpm

at temperature and time interval stated above. Cells were harvested by centrifugation at 4 122 x g and 4°C for 30 min. The supernatant was removed and the cell pellet was frozen at -80°C for further use.

3.15 Protein purification

Cells from large-scale protein expression were thawed on ice and resuspended in 10 mL of lysis buffer supplied with protease inhibitors (SIGMAFAST Protease Inhibitor Cocktail tablets, EDTA-free by Sigma-Aldrich). The sample was then incubated for 20 minutes with DNase I (10 μg/mL) (PanReac AppliChem) and the cells were lysed using LM20 Microfluidizer® Processor (Microfluidics). The cell lysate was clarified by centrifugation at 4°C, 40 700 x g for 1 hour.

3.15.1 HisTrapTM HP affinity chromatography under native conditions

Supernatant from the ultracentrifugation of the cell lysate was used for purification of the reporter from the soluble fraction. ÄKTA™ Pure M2 system (GE Healthcare) fitted with HisTrap™ HP 5 mL column (Cytiva) was washed with 4 column volumes (CV) of double-distilled and de-gassed H_2O. The column was then equilibrated with 4 CV of equilibration buffer, 4 CV of elution buffer, and again 4 CV of equilibration buffer. The sample was loaded using the sample pump with a 1 mL/min flow rate. Upon rising of the UV signal, the flow-through fraction was collected and stored on ice. The column was then equilibrated with an equilibration buffer until the UV signal decreased to the baseline. 10% elution buffer was used to wash away weakly bound proteins and the fraction was collected. The recombinant protein was eluted with an increasing gradient of elution buffer for 20 min until 100% of elution buffer. The UV signal was monitored and the peak was collected in 3 mL fractions. Individual fractions were analyzed using SDS-PAGE as described in chapter 3.12, and protein concentration in each fraction was measured using NanoDrop One (Thermo Scientific).

3.15.2 HisTrap™ HP affinity chromatography under denaturing conditions

The protein pellet obtained from clarification of the cell lysate was dissolved in solubilization buffer and left stirring at 4°C overnight. Next day, the solution was centrifuged again at 4°C, 40 700 x g for 1 hour, and the obtained supernatant was used for the purification. Purification protocol was the same as described above for native state purification only using

buffers containing urea. Collected fractions were analyzed on the SDS-PAGE gel as described in 3.12 with exception of ON and FT fractions, which were 10 times diluted in 1X SDS-PAGE buffer to reduce the concentration of guanidine chloride. All samples were stored at 4°C for further use. Protein concentration in each fraction was measured using NanoDrop One (Thermo Scientific).

3.16 Step down refolding

The sample for refolding was diluted with equilibration buffer to final concentration 0.15 mg/mL, placed into SnakeSkin™ Dialysis Tubing 10.000 MWCO (Thermo Scientific), and clamped. The tubing with the sample was placed into a 1L volumetric cylinder containing 600 mL of buffer A and was left overnight at 4°C on a magnetic stirrer with 300 rpm. After 12 hours, 200 mL of buffer B was added and this step was repeated after another 12 hours. Following every 12 hours, 300 mL of the buffer from the volumetric cylinder was replaced with 300 mL of buffer B, subsequently by buffer C until the final concentration of urea and β-mercaptoethanol was reduced to a minimum. Finally, the sample was removed from the dialysis bag and centrifuged at 40 700 x g, 4°C for 1 hour to get rid of any precipitate. Both pellet (resuspended in 10 mL of dialysis buffer) and supernatant were analyzed by SDS-PAGE. Refolded protein was concentrated using 15 mL Amicon® Ultra-4 Centrifugal Filter unit with 10K cut-off (Merck Millipore) for approximately 45 min at 4 122 x g and 4°C.

3.17 Pilot cleavage studies with NS2B-NS3 protease

To assess if NS2B-NS3 protease cleaves the designed reporter, pilot cleavage studies were performed. TBEV derived recombinant NS2B-NS3 protease was kindly provided by Paulina Duhita Anindita, Ph.D. Two different concentrations of protease and three incubation times were tested, based on the information from the functional studies of the protease [65]. Cleavage reaction was performed in 50 mM Tris buffer supplied with 30% glycerol, pH = 8. Reaction setups are given in Table 13. Mixed reactions were then incubated at 37°C for 30 min, 60 min, and 90 min. The reaction was stopped by the addition of 4X SDS-PAGE buffer followed by boiling at 95°C for 5 min, and samples were then analyzed on 12.5% gel. Obtained cleavage products were cut out from the gel and analyzed by mass spectrometry.

Table 13 – **Set up of cleavage reactions.**

Reagent		
PAmCherry	500 ng	500 ng
NS2B-NS3 protease	0.8 μM	4 μM
50 mM Tris, 30% glycerol (pH = 8)	up to 10 μL	up to 10 μL

3.18 Cell culture

3.18.1 Cell lines and media

Two different mammalian cell lines were used during experiments: African green monkey (*Cercopithecus aethiops)* kidney cells (Vero E6) and baby hamster (*Mesocricetus auratus*) kidney fibroblast cells (BHK-21). Cells were cultivated and maintained at 37°C and 5% CO_2 in Dulbecco's Modified Eagle Medium (DMEM) (Low Glucose without L-glutamine without sodium pyruvate (Biowest, L0064-500)) supplied with 10% bovine fetal serum (BOFES) (Biowest, S1810-100), 1% antibiotics (penicillin-streptomycin solution 100X (Biowest, L0033-020)), 1% L-glutamine (Biowest, X0551-100). The final concentrations were 100 U/mL and 100 μg/mL for the penicillin G and streptomycin respectively and 292 μg/mL for L-glutamine. For the purpose of several experiments, cells were grown in DMEM medium with 10% BOFES without antibiotics or in Gibco™ FluoroBrite™ DMEM (FB DMEM) (Fischer Scientific) supplied with 10% BOFES, 1% antibiotics, and 1% L-glutamine.

3.18.2 Cell preparation

Before each experiment, grown cells were washed twice with 1X PBS and trypsinized with either 0.5 mL (T25 flask) or 1 mL (T75 flask) of Trypsin EDTA 1X in PBS w/o Calcium w/o Magnesium w/o Phenol Red (Biosera). The flask was rotated several times to ensure even coverage and excess trypsin was poured out. Cells were incubated with remaining trypsin for 5 min at 37°C, and consequently, the trypsin was inhibited by addition of 5 mL (T25 flask) or 10 mL (T75 flask) of prewarmed cultivation media with 10% BOFES. Cells were mixed by pipetting and a 50 μL aliquot of cell suspension was removed and dyed with trypan blue solution in a 1:1 ratio for cell counting. Cells were counted in Bürker Chamber and the given amount of cells for each experiment was seeded into respective cultivation vessel.

3.18.3 Transfection

Both Vero E6 and BHK-21 cells were transfected with the gene of interest cloned into pcDNA-pDEST40 using Lipofectamine® 2000 Reagent (Invitrogen). Transfection was performed either directly in the T25 flask for the stable cell line generation or into µ-Dish (Ibidi) to evaluate the expression of the construct by transient transfection.

Cells were plated one day before transfection so they have approximately 70% confluence at the time of transfection (Table 14). Next day, the non-linearized plasmid was diluted in Gibco™ Opti-MEM™ I Reduced Serum Medium (Fischer Scientific) and mixed gently. Lipofectamine® 2000 Reagent was also diluted in Gibco™ Opti-MEM™ I Reduced Serum Medium and incubated at room temperature for 5 minutes. Diluted DNA was then added to the diluted Lipofectamine® 2000 Reagent dropwise, gently mixed by finger flicking, and incubated at room temperature for 20 min. The final DNA to Lipofectamine® 2000 Reagent was 1 µg/1.5 µL. Formed complexes were added into the cultivation vessel with the cells containing medium without antibiotics and incubated for 24 hours at 37°C and 5% CO_2. The exact setup of the reactions for the T25 flask and µ-Dish are shown in Table 15.

Table 14 – **Number of cells seeded for transfection to each cultivation vessel.**

Cell line	T25 flask	µ-Dish
Vero E6	1 500 000	300 000
BHK-21	1 000 000	200 000

Table 15 – **Set up of transfection reactions.**

Reagent	T25 flask	µ-Dish
Lipofectamine® 2000 Reagent	15 µL	4 µL
Opti-MEM medium – Lipofectamine dilution	500 µL	100 µL
DNA	10 µg	4 µg
Opti-MEM medium – DNA dilution	500 µL	100 µL

3.18.4 Antibiotics kill curve

For the establishment of the stable cell lines, the optimal concentration of the selection antibiotic had to be defined. pcDNA-pDEST40 contains a neomycin resistance gene, thus geneticin (G418 - Roche Diagnostics) was used as a selection marker. Cells were plated into a 24-well plate in density 50 000 cells/well in media without antibiotics and were allowed to adhere overnight. The following day, G418 was added in the concentration range reported in

the literature for both cell lines. For Vero E6, G418 concentration ranged from 0.1 mg/mL to 1.4 mg/mL, while for BHK-21 the range was 0.1 mg/mL to 1 mg/mL. Each examined concentration was tested in duplicates. Cells were observed every day to assess cell viability. Medium with fresh G418 was exchanged every 2-3 days. The optimal concentration of G418 was selected as the lowest concentration that killed all the cells within 14 days.

3.18.5 Stable cell line generation

Once the optimal concentration of the selection marker was established, cells were transfected in a T25 flask as described in 3.18.3. 24 hours post-transfection (hpt), the antibiotic selection was initiated with the respective concentration of G418. Cells were incubated at 37°C and 5% CO_2 and medium with fresh G418 was exchanged every 2-3 days. After 2-3 weeks when cells reached 100% confluency following the selection, the cells were frozen and used for further experiments as a polyclonal stable cell line.

3.18.6 Infection with TBEV

For infection of the stable cell lines, a Western-European subtype of tick-borne encephalitis virus - Hypr strain - was used. The virus, multiplied and isolated from Vero E6 cells, was kindly provided by Mgr. Zuzana Beránková. The determined titer of the virus was $6.2x10^7$ PFU/mL.

Cells were seeded, at density 150 000 Vero E6 cells and 100 000 BHK-21 cells per dish, one day before infection in FB DMEM without antibiotics into μ-Dish and left overnight at 37°C and 5% CO_2. The volume of media was reduced to half prior addition of the virus. The virus was added at multiplicity of infection (MOI) 0.25 and 1 (i.e. 0.25 viral particles per cell). Cells were incubated with the virus for 2 hours at 37°C and 5% CO_2. Medium with the virus was then removed, cells washed with 1X PBS and fresh medium was added. Cells were incubated at 37°C and 5% CO_2 for 96 hours.

3.18.7 Fluorescence microscopy

Cells were observed using a wide-field fluorescence microscope. The setup consisted of Sona sCMOS camera (Andor, Oxford Instruments), oil immersion objective (Apo N60X, NA = 1.49, infinity corrected, Olympus), iChrome CLE Compact laser engine (Toptica Photonics), excitation filter TetraQuad Mirror ZT 405/488/561/640rpcr2-UF2 (Chroma

Technology), emission band pass filter FF02-525/40-25 (Semrock) for hMGFP detection and emission band pass filter FF01-60/52-25 (Semrock) for PAmCherry detection.

For fluorescence detection, cells were prepared on μ-Dish as described in 3.18.6. After the infection, fluorescence in cells was detected 24 hours post-infection (hpi), 48 hpi, 72 hpi, and 96 hpi. For observation of the PAmCherry reporter signal, the PAmCherry was photoactivated with 405 nm laser (10 mW) for 10 sec, and the cells were observed using excitation at 561 nm (20 mW) with an exposure time of 25 ms. hMGFP reporter was observed in the cells using excitation by 488 nm laser (20 mW). Due to the significant increase in the fluorescence signal over the course of the observation time, laser intensity and exposure time were varied to obtain well-resolved (unsaturated) cell images. The laser was operated between 25-20% intensity and the exposure time varied from 50 – 250 ms. Images were taken using the Solis Software (Andor, Oxford Instruments) and were analyzed with ImageJ.

Image processing was aimed at showing the localization of the signal in the cells for both reporters and comparison between the not photoactivated and photoactivated state for PAmCherry, thus the images have different colour schemes and are not quantitatively comparable. Scale bar was added to each image or pair of images separately by using a resolution target R3L1S4P (1951USAF, Thorlabs) to calculate the size of one pixel. Quantitative analysis of the PAmCherry signal was performed with data extracted from the raw images. A mask of cytoplasm was constructed for each cell and mean fluorescence intensity was calculated for the given area with ImageJ. Mean fluorescence intensity was also calculated for the background of the image. These two values were used to calculate a signal-to-background ratio (SBR) for each cell prior to and after photoactivation with a 405 nm laser.

4 Results

4.1 Preparation of recombinant cleavage reporters

Several constructs for the production of cleavage reporters were prepared as described in chapter 3. Schematic representation of the constructs with the position of HisTag is shown in Figure 9 (excluding the initial assembly of the reporters in pUC19).

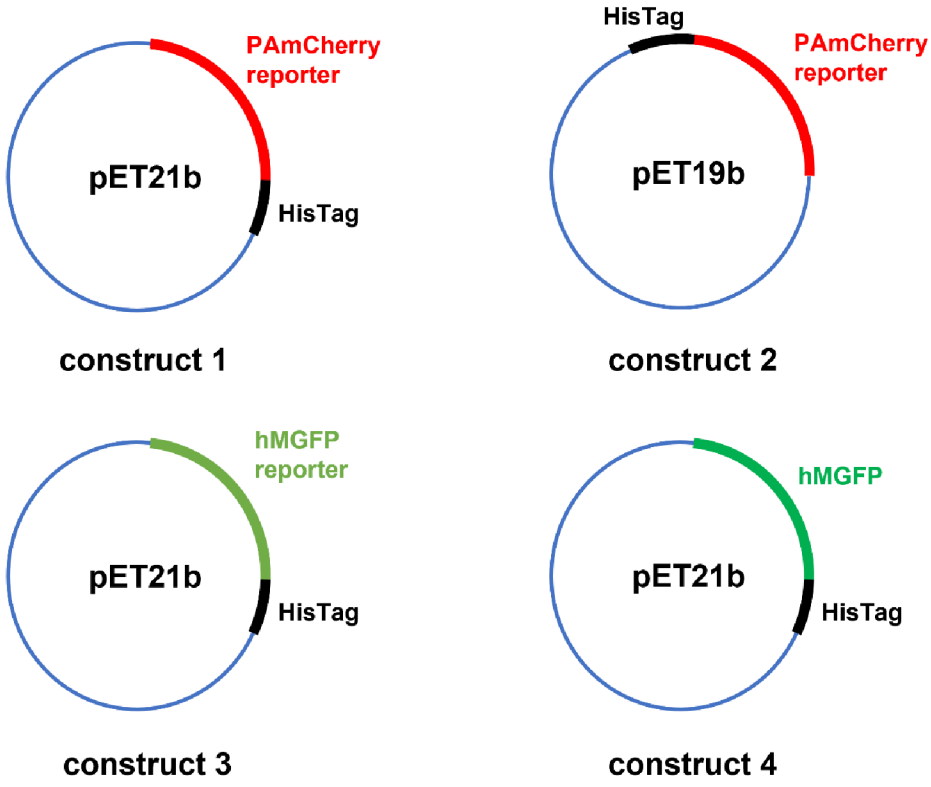

Figure 9 – **Schematic representation of constructs for expression of reporters in competent *E. coli* cells.** pET21b plasmid carries C-terminal HisTag, while pET19b has N-terminal HisTag.

4.1.1 Cloning of cleavage reporters

All sets of primers were tested for optimal annealing temperature by gradient PCR. The optimal annealing temperature for each primer pair is shown in Table 16.

Table 16 – **Optimal annealing temperatures for each set of primers.**

Amplicon	Primer 1	Primer 2	Destination vector	Optimal annealing temperature [°C]
PAmCherry_rep_1	pPAmCherry_linker_R	pPAmCherry_F	pUC19	53
PAmCherry_rep_2	pPAmCherry_rep_CR_NdeI_F	pPAmCherry_rep_CR_XhoI_R	pET21b	60
PAmCherry_rep_3	pPAmCherry_rep_CR_NdeI_F	pPAmCherry_rep_CR_STOP_R	pET19b	60
hMGFP	hMGFP_F	hMGFP_R	pUC19	70
pUC19_inhib	pUC19_inhib_F	pUC19_inhib_ R	pUC19	75
hMFGP_rep	hMGFP_rep_F	pPAmCherry_rep_CR_XhoI_R	pET21b	63
hMGFP_control	hMGFP_rep _F	hMGFP_control_R	pET21b	60

This temperature was used for amplification of the constructs by Q5® High Fidelity DNA polymerase with 3'→ 5' exonuclease activity providing an ultra-low error rate. The success of the PCR amplification and correct construct sizes (PAmCherry_rep: 822 bp, hMGFP: 681 bp, pUC19_inhib: 2800 bp, hMGFP_rep: 795 bp) were verified by agarose gel electrophoresis (Figure 10). Each amplicon was purified from the gel and obtained in the concentration given in Table 17.

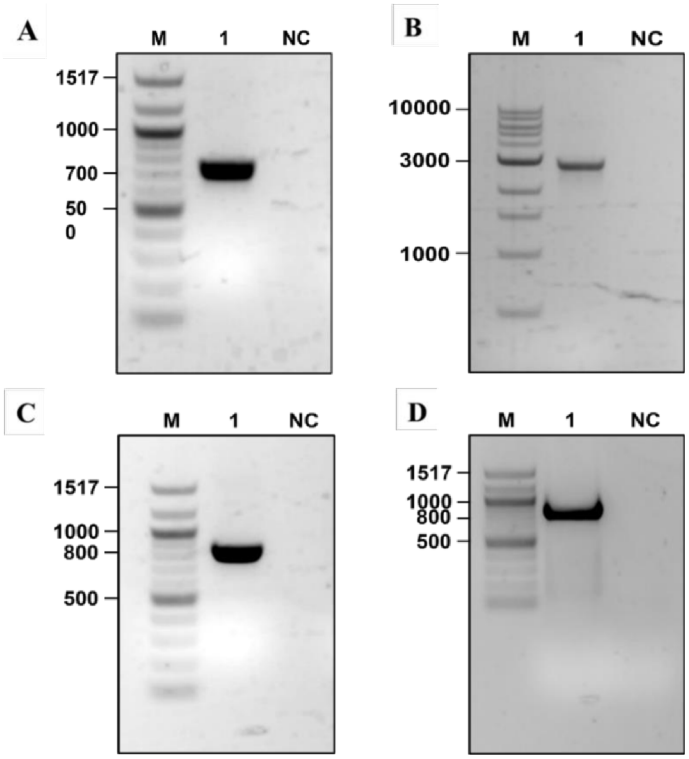

Figure 10 – **Gel electrophoresis of Q5® Polymerase PCR products.** A: 1 – hMGFP, B: 1 – pUC19 containing inhibitory peptide, C: 1 – hMGFP reporter, D: 1 – PAmCherry reporter. M – 100 bp DNA Ladder (New England Biolabs), NC – negative control.

Table 17 – **DNA concentration of all amplicons obtained from PCR with Q5® Polymerase.**

Amplicon	Destination vector	DNA concentration [ng/uL]
PAmCherry_rep_1	pUC19	25
PAmCherry_rep_2	pET21b	82.3
PAmCherry_rep_3	pET19b	104
hMGFP	pUC19	224
pUC19_inhib	pUC19	88
hMFGP_rep	pET21b	310.3
hMGFP_control	pET21b	243.8

The amplicons were inserted into respective plasmids either by Gibbson assembly (assembly of the constructs into pUC19) or restriction digestion (pET21b and pET19b). NEB® 5-alpha Competent *E. coli* cells were transformed with the resulting reaction mixture. 15 colonies were picked up the next day and analyzed for presence of the gene of interest by colony PCR. In all cases, positive colonies were identified by presence of DNA band of the correct size. An example of colony PCR agarose gel electrophoresis of hMGFP reporter in pET21b is shown in Figure 11. Data for the rest of the constructs are not shown.

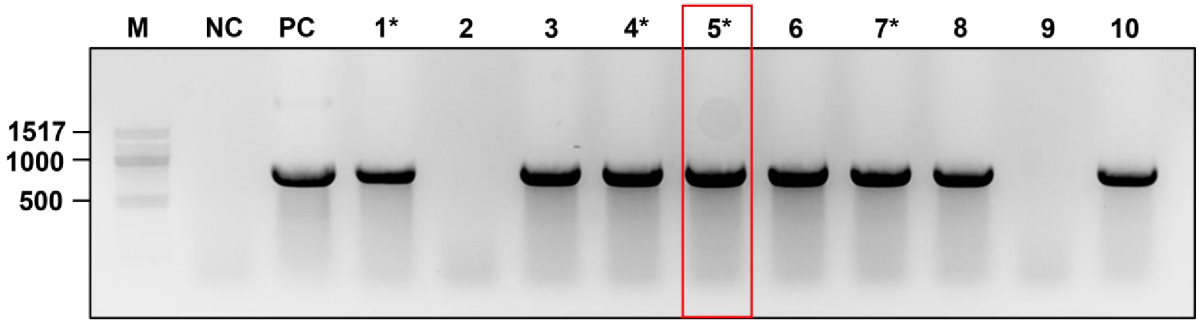

Figure 11 – **Gel electrophoresis of colony PCR of hMGFP reporter in pET21b.** M – 100 bp DNA Ladder (New England Biolabs). NC – negative control with no DNA template. PC – positive control, added DNA template of pure plasmid with the insert. Samples marked with an asterisk were sent for sequencing, the red marked sample was used to prepare maxiprep.

Minipreps were prepared from the positive colonies and sequenced. For each construct, one sequence-verified clone was chosen and maxiprep was prepared. The obtained plasmids were either used as the template for re-cloning of the construct into a different plasmid or directly for transformation into expression strains of *E. coli*.

4.1.2 Production of cleavage reporter in competent *E. coli* cells

Pilot expression was performed with both reporters to find optimal conditions for recombinant protein production. Several strains of competent *E. coli* were tested as well as two different temperatures (30° and 18°C). Production at 30°C was sampled at time intervals

of 2h, 4h, and 6h while production at 18°C was sampled at 3h, 6h, and 24h (overnight). Estimated molecular weights excluding His-Tag for PAmCherry reporter and hMGFP reporter are 30.8 kDa and 30 kDa, respectively.

PAmCherry reporter was produced in two strains: BL21(DE3) and BL21-CodonPlus, using two different plasmids pET21b with C-terminal His-tag (construct 1, see Figure 9) and pET19b with N-terminal His-tag (construct 2). Expression of construct 2 showed no production at all in either of the conditions (data in Supplement). Therefore, further work with this construct was discontinued. On the other hand, the expression of construct 1 showed significant protein production in both cell types and temperatures in the insoluble fraction (Figure 12 and 13). As there was no detectable protein in the soluble fraction, production in BL21-CodonPlus cells at 30°C for 6 hours was chosen to be suitable for large-scale production and subsequent denaturation purification and refolding.

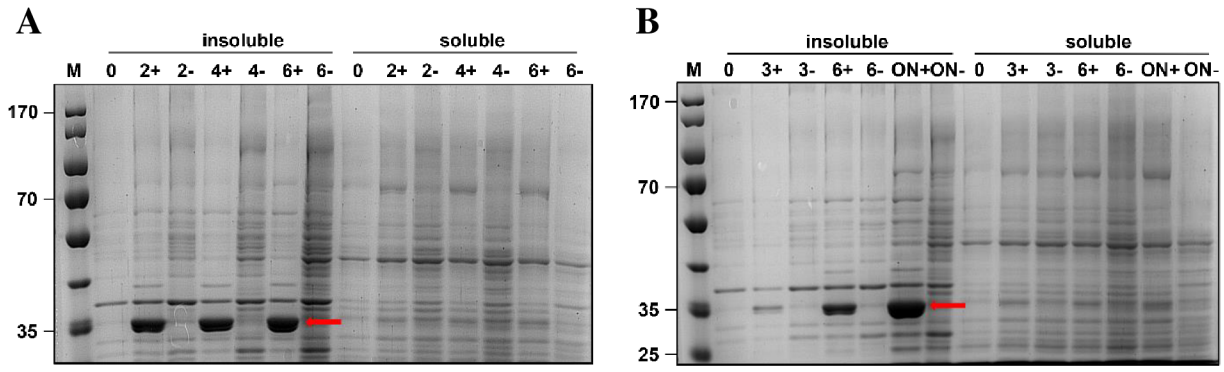

Figure 12 – **SDS-PAGE analysis of PAmCherry reporter expression in pET21b in BL21-CodonPlus cells.** A – 30°C, B – 18°C. M – PageRuler Prestained Protein Ladder (Thermo Fischer). – sign indicates uninduced culture, + sign indicates induced culture, each number represents an hour of collection of the sample after the induction.

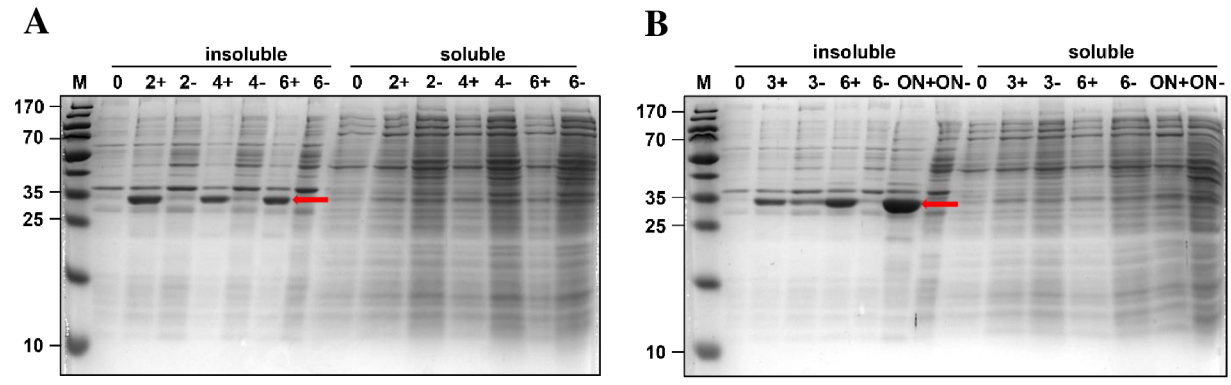

Figure 13 – **SDS-PAGE analysis of PAmCherry reporter expression in pET21b in BL21(DE3) cells.** A – 30°C, B – 18°C. M – PageRuler Prestained Protein Ladder (Thermo Fischer). – sign indicates uninduced culture, + sign indicates induced culture, each number represents an hour of collection of the sample after the induction.

hMGFP reporter production was tested using only pET21b plasmid (construct 3) in four different *E. coli* strains: BL21(DE3), BL21-CodonPlus, One Shot® BL21(DE3)pLysS, and Rosetta-gami® 2(DE3). Production in BL21(DE3) and BL21-CodonPlus yielded protein in the insoluble fraction at both temperatures (Figure 14 and 15), generally with no protein production in the soluble fraction. However, a weak protein band of hMGFP reporter size was found in the soluble fraction of production in BL21-CodonPlus at 18°C, at time point ON+ (marked with a red rectangle), thus this sample was analyzed with Western blot. Western blot analysis (Figure 16) with antibodies against His-Tag confirmed the presence of the protein of interest in the soluble fraction.

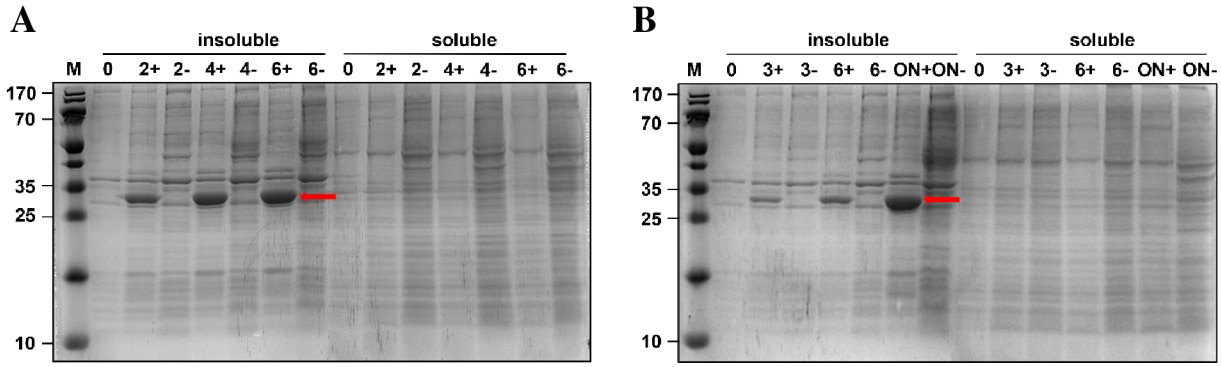

Figure 14 – **SDS-PAGE analysis of hMGFP reporter expression in pET21b in BL21(DE3) cells.** A – 30°C, B – 18°C. M – PageRuler Prestained Protein Ladder (Thermo Fischer). – sign indicates uninduced culture, + sign indicates induced culture**,** each number represents an hour of collection of the sample after the induction.

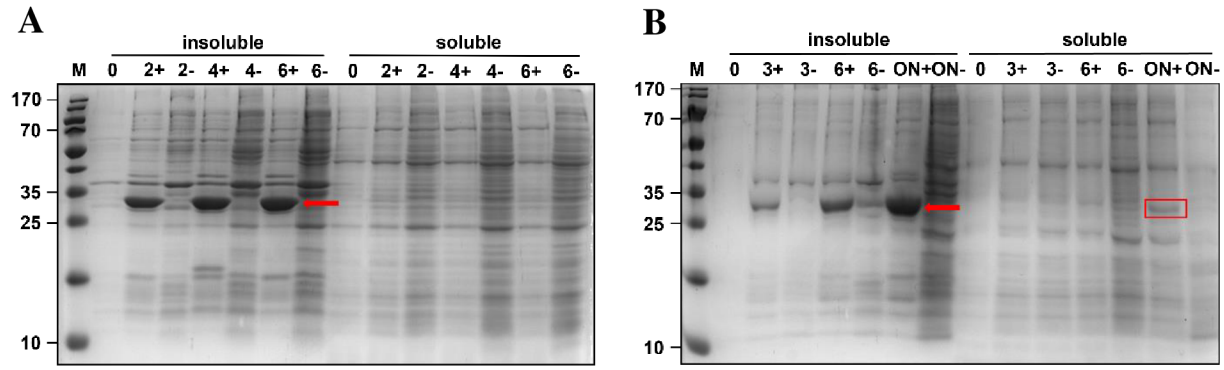

Figure 15 – **SDS-PAGE analysis of hMGFP reporter expression in pET21b in BL21- CodonPlus cells.** A – 30°C, B – 18°C. M – PageRuler Prestained Protein Ladder (Thermo Fischer). – sign indicates uninduced culture, + sign indicates induced culture**,** each number represents an hour of collection of the sample after the induction.

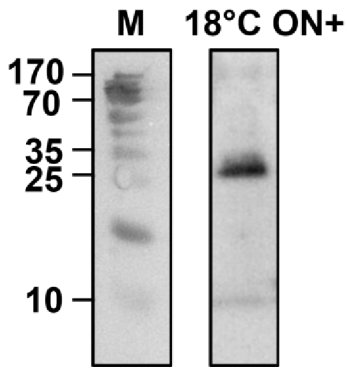

Figure 16 – **Western blot analysis of hMGFP reporter expression in BL21- CodonPlus cells at 18°C ON+ sample using anti-His antibody.** M – PageRuler Prestained Protein Ladder (Thermo Fischer).

Production of construct 3 in One Shot® BL21(DE3)pLysS and Rosetta-gami® 2(DE3) showed a similar pattern as above as all the protein was found in the insoluble fraction (data in Supplement). Based on these results, BL21-CodonPlus cells at temperature of 18°C and overnight production were chosen as a suitable condition for large-scale production of hMGFP reporter to attempt purification from soluble fraction as well as denaturing purification followed by refolding.

In order to see if the influenza inhibition peptide might have an effect on the accumulation of the produced reporter in the inclusion bodies, hMGFP fluorescent protein was produced in BL21(DE3) cells (construct 4). Interestingly, the production of only hMGFP protein lacking the quenching peptide yielded a significant amount of protein in soluble fraction at both temperatures (Figure 17). At 18°C majority of the protein was found in the soluble phase, which implies lower temperature is required to obtain properly folded hMGFP. This suggests that the quenching peptide indeed has an effect on the presence of the hMGFP reporter in the insoluble fraction.

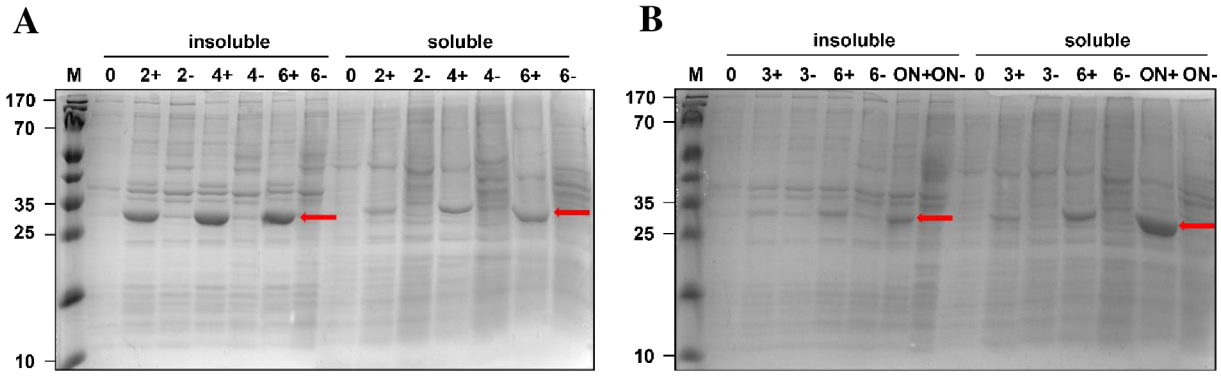

Figure 17 – **SDS-PAGE analysis of hMGFP protein expression in pET21b in BL21- CodonPlus cells.** A – 30°C, B – 18°C. M – PageRuler Prestained Protein Ladder (Thermo Fischer). – sign indicates uninduced culture, + sign indicates induced culture, each number represents an hour of collection of the sample after the induction.

4.1.3 Purification of cleavage reporter

PAmCherry reporter (construct 1) was purified using its C-terminal His-Tag via immobilized metal affinity chromatography (IMAC) under denaturing conditions fitted with HisTrap™ HP column. Harvested cells were lysed in a microfluidizer and soluble/insoluble fractions were separated by centrifugation. The insoluble fraction from large-scale production was solubilized and centrifuged to clarify the solution of insoluble parts. The supernatant was purified via IMAC using a gradient elution of protein from the column. 3 mL peak fractions were automatically collected and analyzed with SDS-PAGE (Figure 18). In the two collected fractions (1 and 2), the protein concentration was measured and yielded 0.639 mg/mL (A260/A280 = 0.59) and 0.239 mg/mL (A260/A280 = 0.5), respectively.

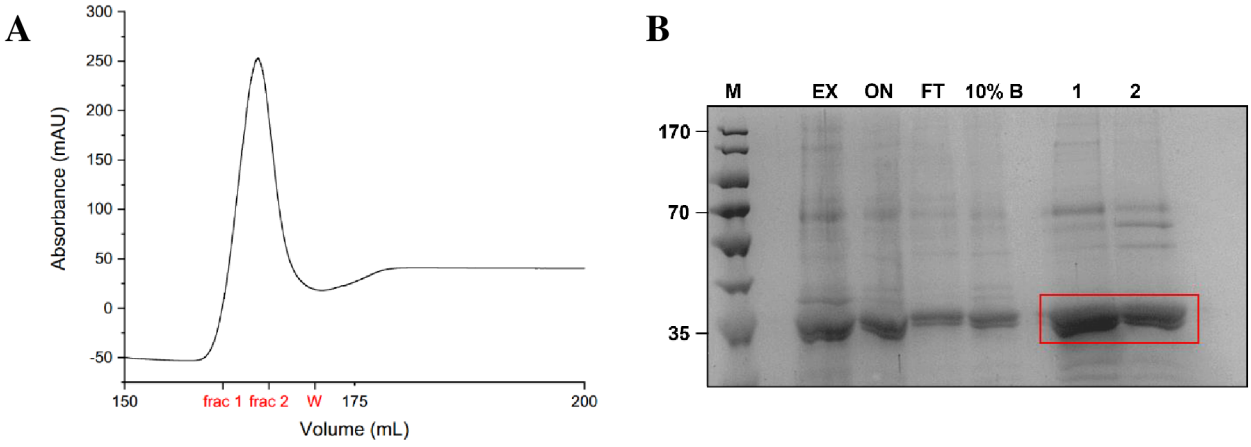

Figure 18 – **Denaturing purification of PAmCherry reporter.** A – Purification chromatogram, showing collected fractions, frac 1 – fraction 1, frac 2 – fraction 2, W – waste. B – SDS-PAGE analysis of IMAC purification. M – PageRuler Restrained Protein Ladder (Thermo Fischer). EX – sample taken after extraction from inclusion bodies, ON – sample loaded onto column, FT – flow-through fraction, 10% B – eluate with 10% elution buffer, 1 and 2 – eluted fractions with PAmCherry reporter.

hMGFP reporter was produced in a large scale (construct 3) using the conditions which showed the potential presence of the reporter in the soluble fraction. Cells were lysed and fractions were separated as described above. At first, the collected supernatant was loaded onto HisTrap™ HP column and the reporter was purified under native conditions with IMAC. However, there was little to no protein peak during elution and SDS-PAGE analysis confirmed that there are no observable bands for the purified reporter in either of the collected fractions (data in Supplement). Thus, the hMGFP reporter was purified from inclusion bodies using denaturing IMAC like the PAmCherry reporter as described above. Figure 19 shows the chromatogram and the SDS-PAGE analysis of the collected fractions. The concentration of the protein in the fractions was measured and is given in Table 18.

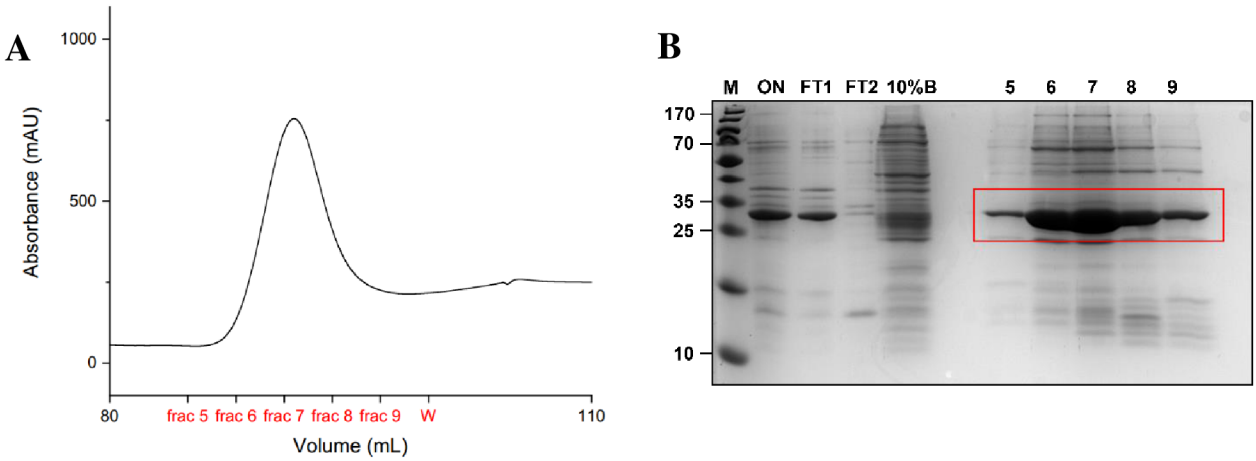

Figure 19 – **Denaturing purification of hMGFP reporter.** A – Purification chromatogram, showing collected fractions, frac 5 – fraction 5, frac 6 – fraction 6, frac 7 – fraction 7, frac 8 – fraction 8, frac 9 – fraction 9, W – waste. B – SDS-PAGE analysis of IMAC purification. M – PageRuler Restrained Protein Ladder (Thermo Fischer). ON – sample loaded onto the column, FT1 – flow-through fraction 1, FT2 – flow-through fraction 2, 10% B – eluate with 10% elution buffer, 5 – 9 eluted fractions with hMGFP reporter.

Table 18 – **hMGFP reporter concentration in collected fractions.**

Fractions	Concentration [mg/mL]	A260/A280
5	0.047	1.37
6	1.114	0.63
7	2.281	0.60
8	0.738	0.63
9	0.375	0.67

4.1.4 Step-down refolding of cleavage reporter

Fractions from denaturing purifications for each reporter were prior refolding diluted to a suitable concentration of 0.15 mg/mL with equilibration buffer. The diluted sample was dialyzed until there was no urea and β-mercaptoethanol present. The supernatant was separated from precipitate by centrifugation and content of both fractions was analyzed by SDS-PAGE analysis (Figure 20 and 21). Protein bands around 30 kDa were present in both soluble and insoluble fractions for PAmCherry reporter. As can be seen from Figure 20, a sufficient amount of refolded protein was obtained in the soluble fraction, comparable to the concentration prior to refolding. Protein concentration in the soluble fraction was measured to be 0.123 mg/mL, which was further concentrated using Amicon® Ultra 15 mL Centrifugal filters (10K cut-off) to 0.246 mg/mL. The majority of the hMGFP reporter was present in the precipitate, thus further experiments were discontinued.

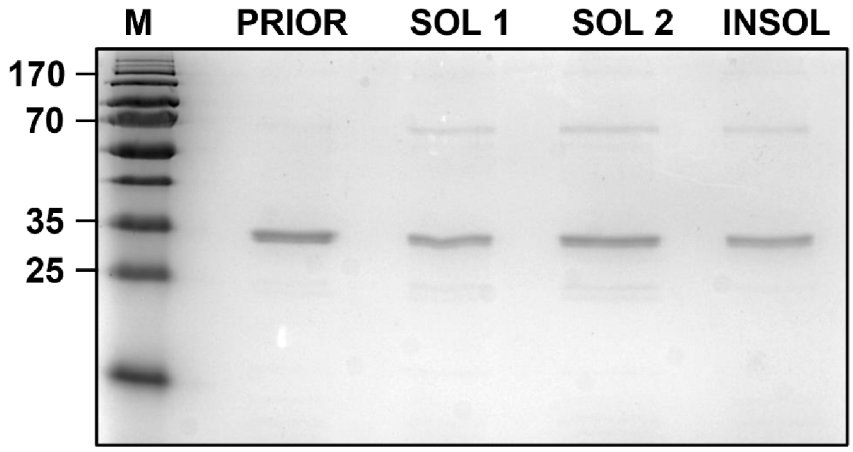

Figure 20 – **SDS-PAGE analysis of PAmCherry reporter refolding.** M – PageRuler Prestained Protein Ladder (Thermo Fischer). PRIOR – diluted sample prior to refolding, SOL 1 – soluble fraction after refolding 10 μL sample loaded, SOL 2 – soluble fraction after refolding 20 μL sample loaded, INSOL – insoluble fraction after refolding.

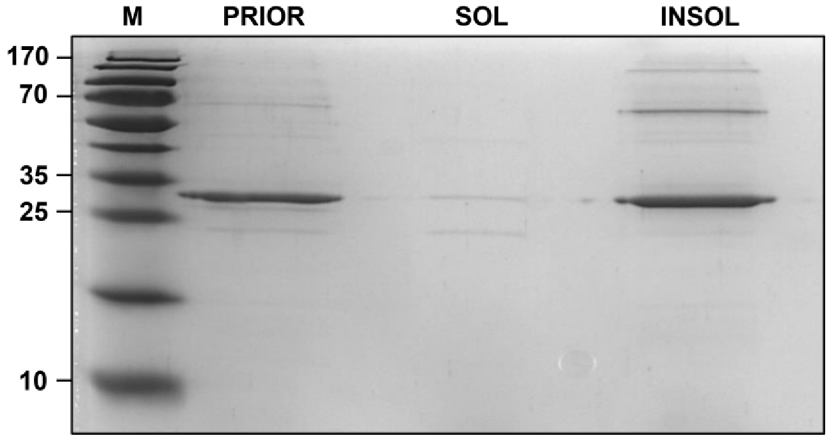

Figure 21 – **SDS-PAGE analysis of hMGFP reporter refolding.** M – PageRuler Prestained Protein Ladder (Thermo Fischer). PRIOR – diluted sample prior to refolding, SOL – soluble fraction after refolding, INSOL – insoluble fraction after refolding.

4.1.5 Pilot cleavage study with TBEV NS2B-NS3 protease

Refolded PAmCherry cleavage reporter was tested for the cleavage reaction with TBEV derived NS2B-NS3 protease. Different concentrations of protease were tested, with 4 μM NS2B-NS3 protease being identified as the most suitable for assays [65]. As can be seen from Figure 22, three distinct bands were observed in each cleavage reaction (red rectangle). The largest band corresponds to the size of the uncut cleavage reporter, which is followed by two smaller cleavage products. In order to differentiate which cleavage product is the one of interest, bands were cut out from the gel and further analyzed by mass spectrometry (performed by Mgr. Filip Dyčka, Ph.D.). Mass spectrometry analysis showed that these three bands are indeed the PAmCherry cleavage reporter, but it was not possible to identify the exact cleavage sites very likely due to the lack of presence of arginine or lysine residues in

the quenching peptide sequence. However, based on the peptide fragments captured during the analysis the results suggest the first larger cleavage product is the result of cleavage at the designed TBEV NS2B-NS3 cleavage site (data shown in Supplement).

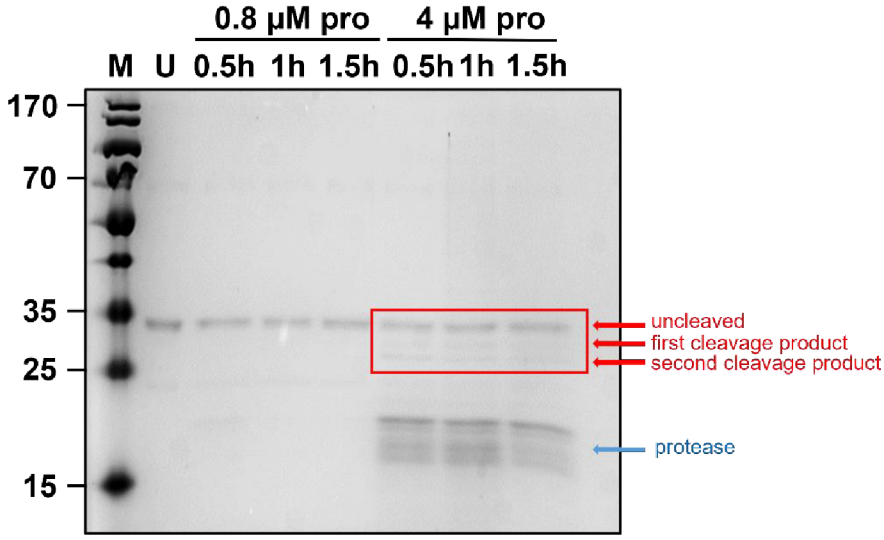

Figure 22 – **SDS-PAGE analysis of PAmCherry cleavage study with TBEV NS2B-NS3 protease.** M – PageRuler Prestained Protein Ladder (Thermo Fischer). U – uncut PAmCherry.

4.2 Cell culture

4.2.1 Plasmid preparation for in cell studies

Primers for the preparation of plasmids for mammalian cells were also tested by gradient PCR for optimal annealing temperature. The optimal annealing temperature for both sets of primers for cloning the reporters into pDONR207 vector was determined to be 60°C. Once the constructs were assembled in pUC19 plasmid, they were amplified with Q5® High Fidelity DNA polymerase using the annealing temperature stated above and purified from the gel. The PAmCherry reporter and hMGFP reporter were obtained in concentration 101 ng/µL and 287.7 ng/µL, respectively. The genes were inserted into the pDONR207 vector by BP reaction with Gateway™ BP Clonase™ II Enzyme mix and transformed into NEB® 5-alpha Competent *E. coli*. The presence of gene of interest in the plasmid was verified with colony PCR. An example of 1% agarose gel electrophoresis analysis of colony PCR of hMGFP reporter in pDONR207 is shown in Figure 23.

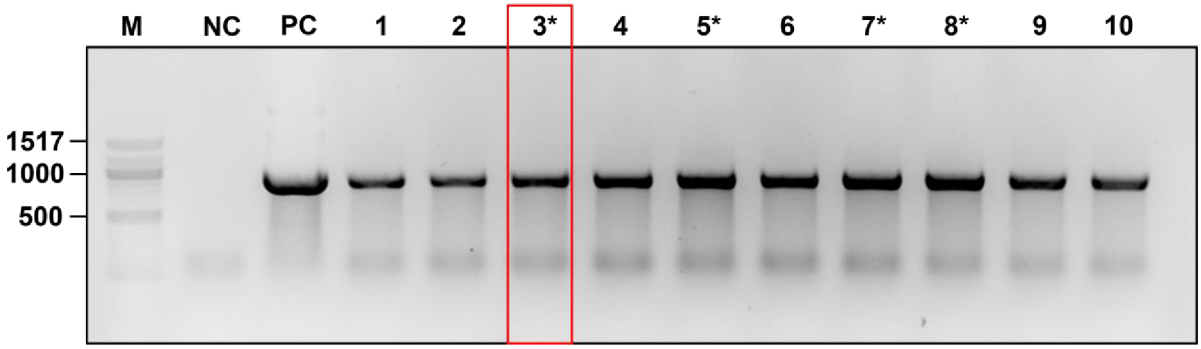

Figure 23 – **Gel electrophoresis of colony PCR of hMGFP reporter in pDONR207.** M – 100 bp DNA Ladder (New England Biolabs). NC – negative control with no DNA template. PC – positive control, added DNA template of pure plasmid with the insert. Samples marked with an asterisk were sent for sequencing, the red marked sample was used to prepare maxiprep.

Sequencing confirmed that the genes of interest were present in the pDONR207 vector without mutations and frameshift, thus for each reporter a maxiprep from one clone was prepared to use for further experiments. Reporter genes were transferred into pcDNA-pDEST40 expression vector using Gateway™ LR Clonase™ II Enzyme mix and transformed into NEB® 5-alpha Competent *E. coli*. Successful transfer of the genes into new plasmids was too verified by colony PCR (Figure 24).

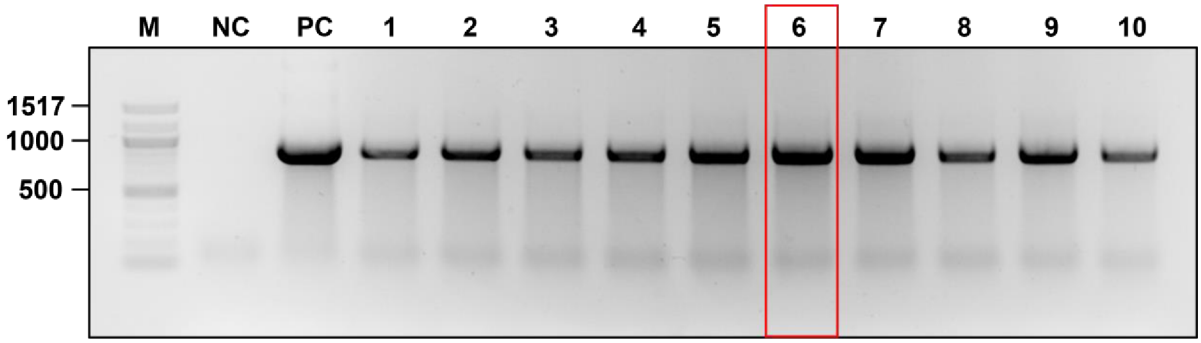

Figure 24 – **Gel electrophoresis of colony PCR of hMGFP reporter in pcDNA-pDEST40**. M – 100 bp DNA Ladder (New England Biolabs). NC – negative control with no DNA template. PC – positive control, added DNA template of pure plasmid with the insert. Red marked sample was used to prepare maxiprep.

Once the presence of gene of interest in pcDNA-pDEST40 vector was confirmed, maxiprep of both reporters in pcDNA-pDEST40 were prepared and additionally purified by ethanol precipitation to ensure extra clean plasmids for transfection into mammalian cells.

4.2.2 Antibiotic kill curve

Prior to transfection of both reporter constructs into the mammalian cells, the sensitivity of both chosen cell lines to geneticin (G418) was tested to find optimal concentration for the establishment of stable cell lines expressing the reporters. Cells were

plated in 24-well plates in density 50 000 cells/well, treated with increasing concentrations of G418, and observed for viability in the course of 14 days. Figure 25 shows the observations of the viability of the cells. The optimal concentration of G418 was taken as the lowest concentration of G418 that killed all the cells within 14 days. Based on these results, the concentration of 0.4 mg/mL for Vero E6 cells and 0.25 mg/mL for BHK-21 (data not shown) was determined as optimal and was used in further experiments.

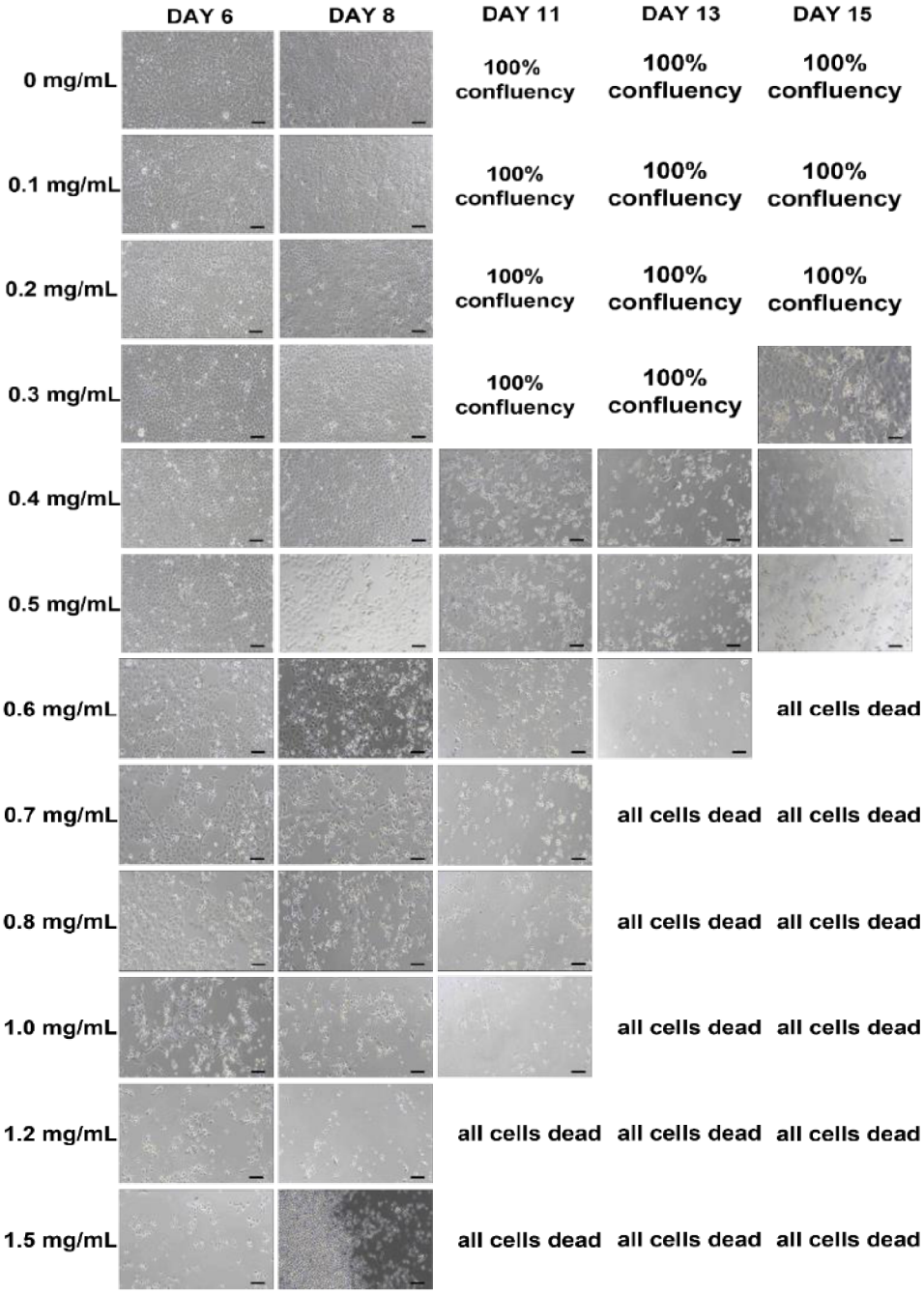

Figure 25 – **The viability of Vero E6 cells under increasing concentration of G418.** Day number marks the day after the addition of G418. Scale bar represents 100 μm.

4.2.3 Evaluation of PAmCherry fluorescence in cells upon TBEV infection

The ability of the PAmCherry reporter to respond to TBEV infection was evaluated by fluorescence microscopy. The stable cell lines were infected with Hypr strain of TBEV at MOI of 0.25 and 1 and observed at regular 24 hours intervals. PAmCherry was photoactivated with a laser of 405 nm wavelength for 10 sec and the signal was observed upon excitation at 561 nm. The resulting images of PAmCherry fluorescence in Vero E6 and BKH-21 cell lines are shown in Figure 26 and 27, respectively. As can be seen from these images, a significant increase in fluorescence compared to the not photoactivated state was observed in all cases. Upon the TBEV infection, the localization of the signal from vesicles changed into the whole cytoplasm of the cell, which signifies the response to the replication of the virus. These images are intended to show the change in localization and increase in fluorescence between the non-photoactivated and photoactivated state but are not quantitatively comparable with one another due to different colour scheme. Non-transfected cell control was imaged under the same condition to observe the level of autofluorescence in each cell line (data in Supplement). Quantitative analysis was performed by extracting mean fluorescence intensity data from raw images and plotting them as a signal-to-background ratio (SBR) of not photoactivated and photoactivated PAmCherry (Figure 28). Figure 28 shows the rise of fluorescence in both cell lines compared to the control cell with no virus, starting at 48hpi for Vero E6 cells and at 72hpi for BHK-21 cells. An increase of SBR of approximately 2 could be observed at 72hpi for both types of cells compared to the non-photoactivated PAmCherry as well as compared to the control cells without any TBEV. This finding suggests a correlation of increase in PAmCherry fluorescence with increased activity of the NS2B-NS3 protease and thus with the replication of TBEV in the cells over the course of infection. BHK-21 cells could not be monitored longer than for 72hpi due to extensive dying from the TBEV infection. A similar trend in the increase of fluorescence was observed for both used MOI values in both cell lines (data for MOI = 1 given in Supplement).

Comparison of both cell lines and multiplicity of infections, as shown in Figure 29, demonstrates a significant rise in fluorescence in all cases. This implies that the PAmCherry reporter could provide a valuable tool for tracking the virus replication in the living cells.

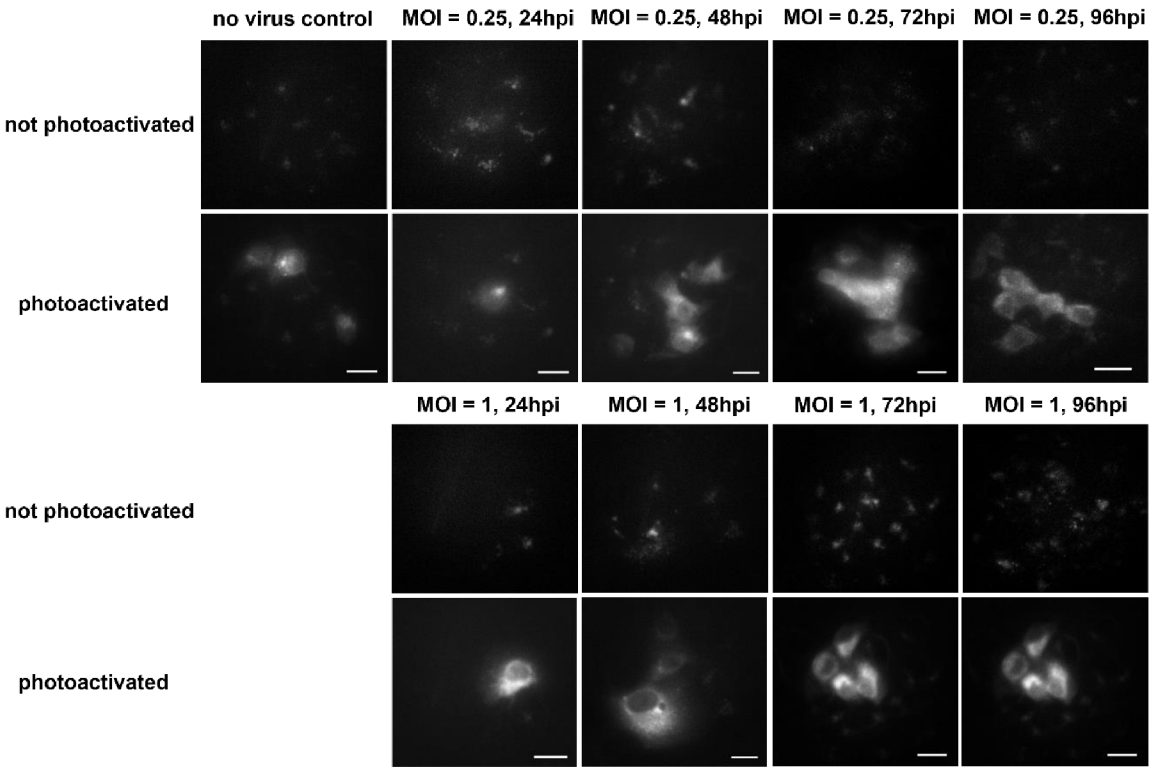

Figure 26 – **PAmCherry fluorescence in Vero E6 cells monitored over time.** No virus control represents the stable cell lines expressing the reporter, which has not been treated with TBEV. Individual images of photoactivated PAmCherry have a different colour scheme and thus are not quantitatively comparable. Scale bar represents 20 μm.

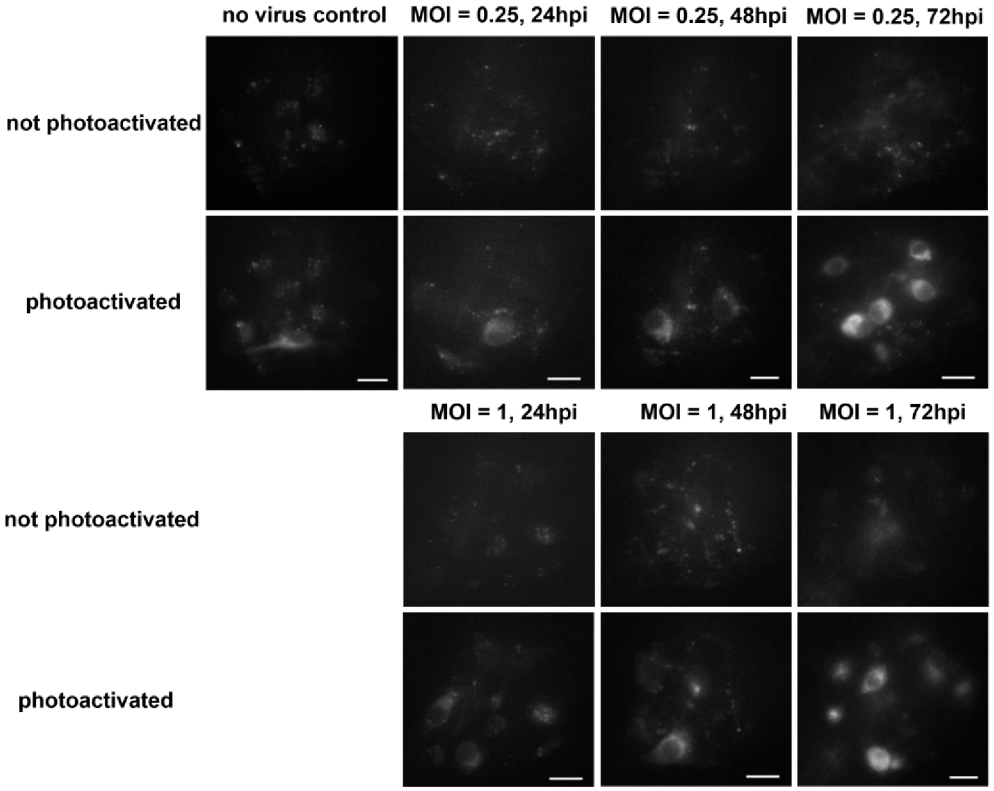

Figure 27 – **PAmCherry fluorescence in BHK-21 cells monitored over time.** No virus control represents the stable cell lines expressing the reporter, which has not been treated with TBEV. Individual images of photoactivated PAmCherry have a different colour scheme and thus are not quantitatively comparable. Scale bar represents 20 μm.

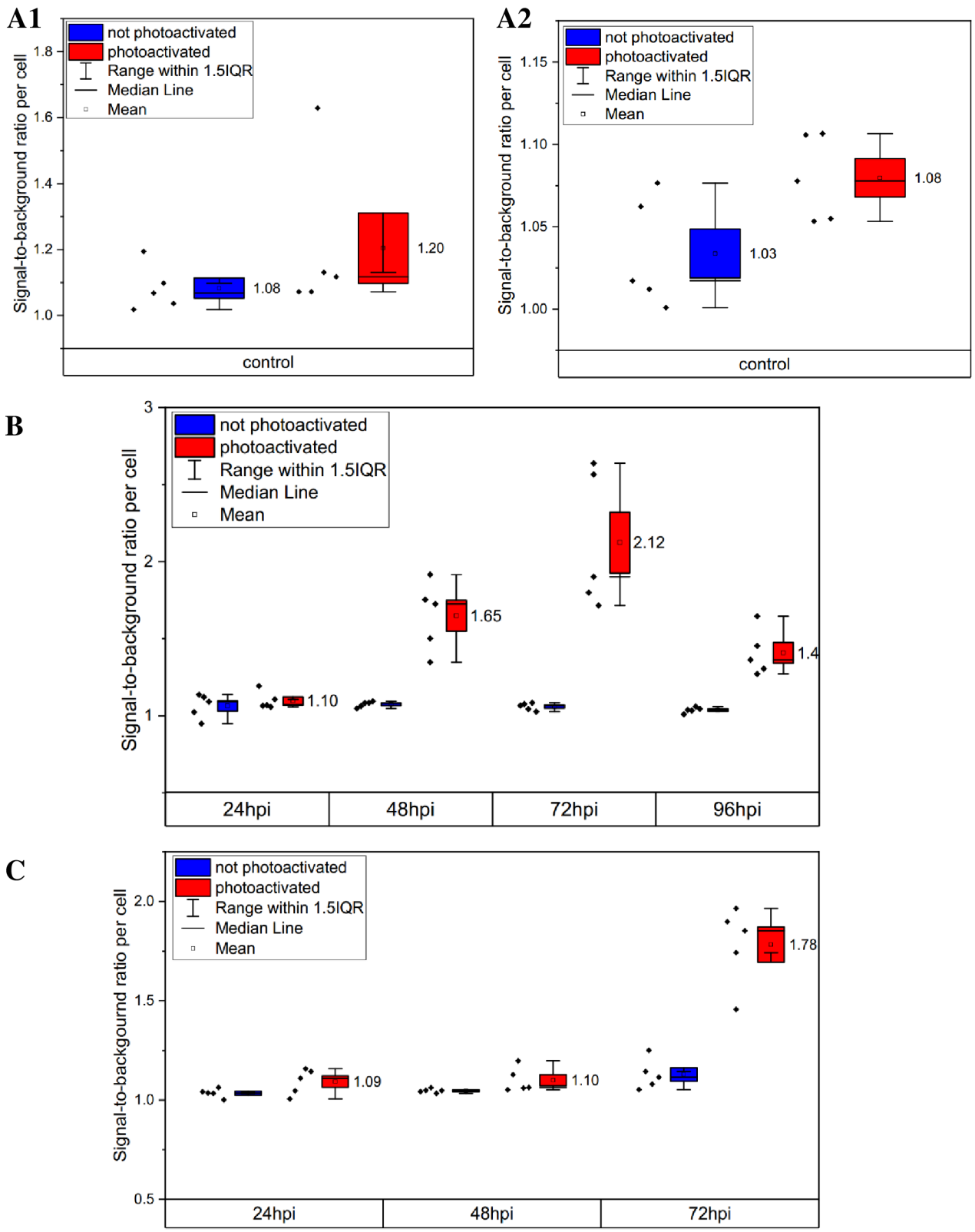

Figure 28 – **Fluorescence intensity analysis of PAmCherry in cells comparing not photoactivated and photoactivated PAmCherry.** A1 – control Vero E6 cells, A2 – control BHK-21 cells, B – Vero E6, MOI = 0.25, C – BHK-21 cells, MOI = 0.25, control represents sample cells expressing reporter but without the presence of TBEV. Data for MOI = 1 are given in Supplement.

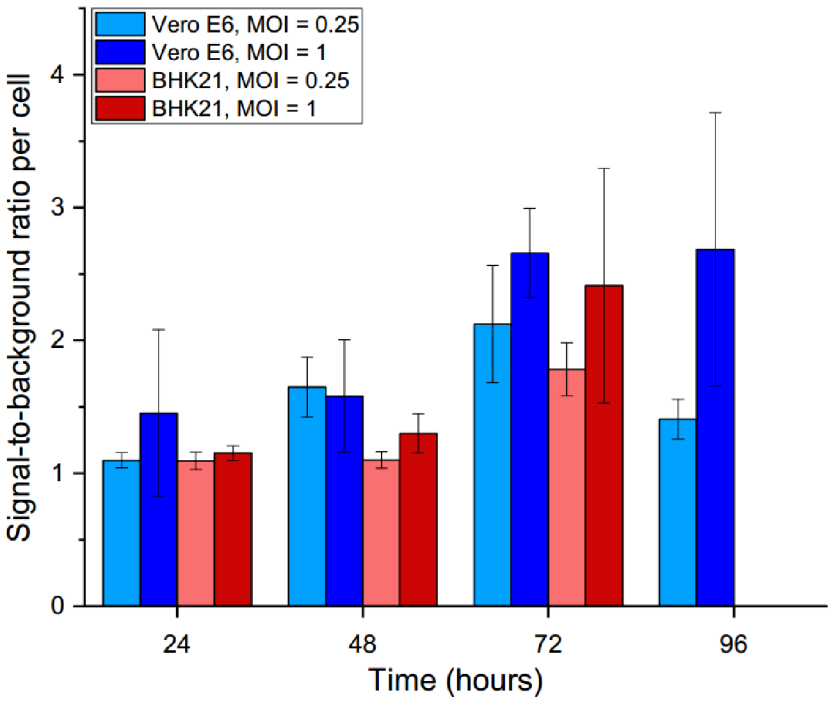

Figure 29 – **Comparison of calculated signal-to-background ratio for all used cell types and MOI values.** Only the SBR of photoactivated PAmCherry is shown. The data are expressed as mean values ± SD.

4.2.4 Evaluation of hMGFP fluorescence in cells upon TBEV infection

Fluorescence of the hMGFP reporter in cells undergoing TBEV infection was monitored in the same way as the PAmCherry reporter. The signal was observed upon excitation with a laser of 488 nm wavelength. Due to the large increase in the fluorescence signal the parameters of the observation (laser intensity and exposure time) had to be changed several times and therefore the quantification of the signal from the images was not possible. As can be seen from the images (Figure 30 and 31) the background signal in the cells not treated with TBEV is large at all time points, and it is larger for Vero E6 cell line. Nonetheless, an increase in fluorescence in response to the TBEV infection can be observed visually in BHK-21 cells as the localization of the signal changes from confined vesicles to the whole volume of the cytoplasm. The trend in the increase of the signal appears to be similar for both MOI values. As before, the observation of the BHK-21 cell line was limited to 72hpi due to extensive dying of the cells.

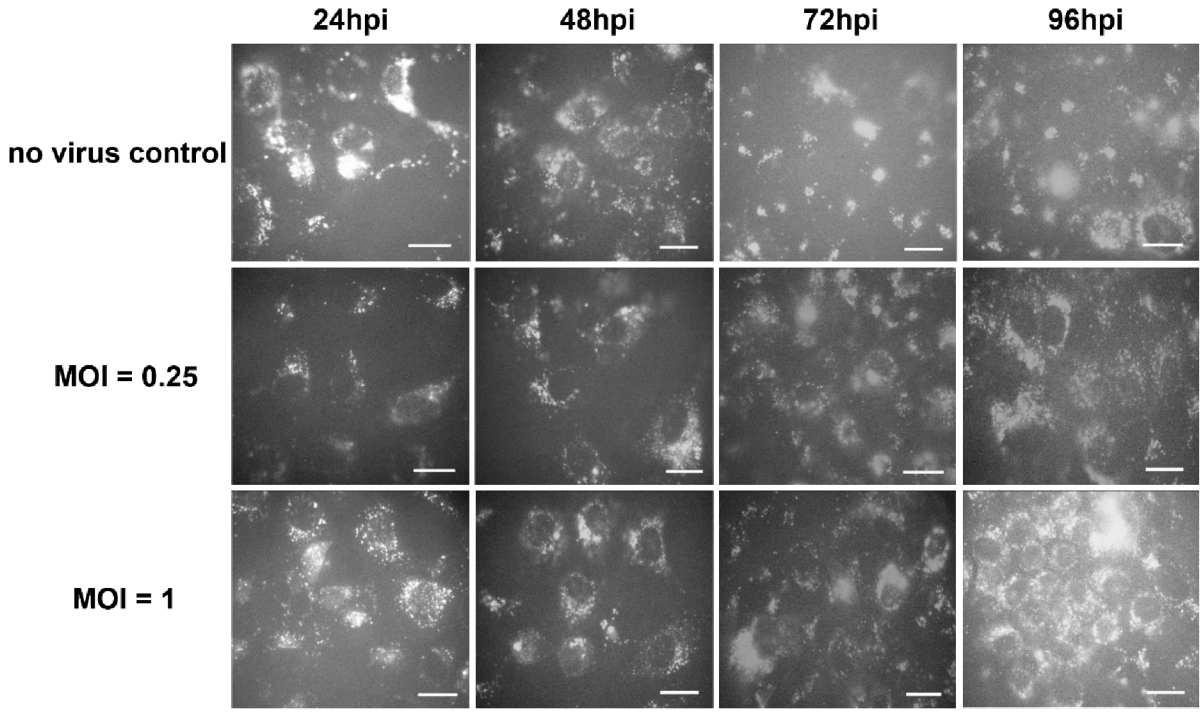

Figure 30 – **hMGFP fluorescence in Vero E6 cells monitored over time.** No virus control represents the stable cell lines expressing the reporter, which has not been treated with TBEV. Scale bar represents 20 μm.

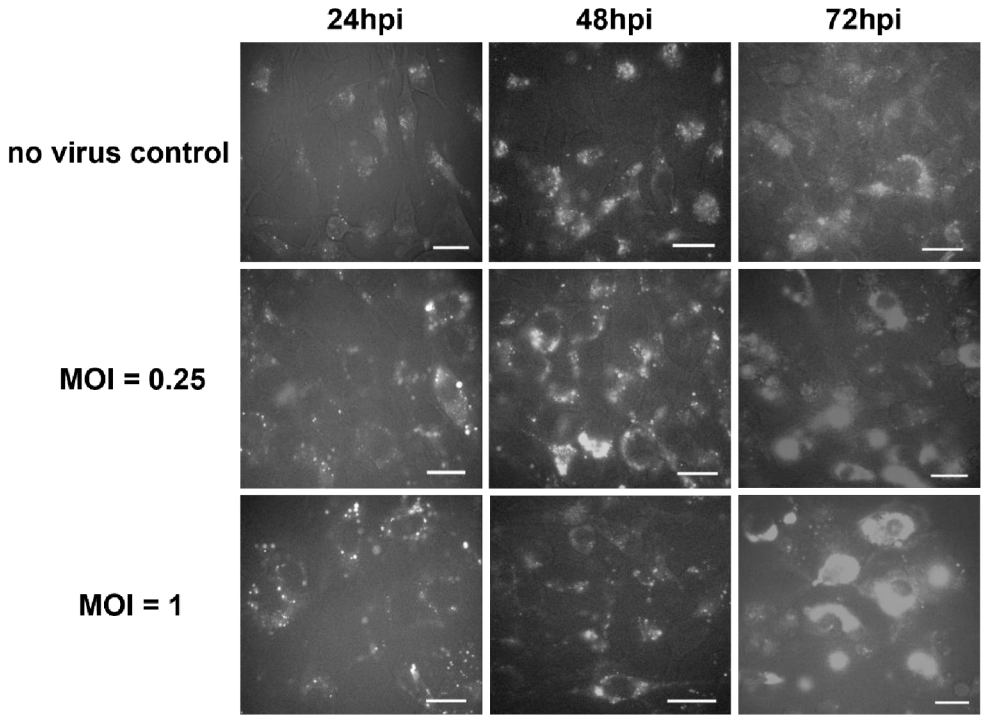

Figure 31 – **hMGFP fluorescence in BHK-21 cells monitored over time.** No virus control represents the stable cell lines expressing the reporter, which has not been treated with TBEV. Scale bar represents 20 μm.

5 Discussion

With the increasing incidence of flaviviral diseases and a lack of specific antiviral treatment, it is important to understand the virus-host interactions to find new therapeutic targets for drug design. Cell culture models are essential to study these diseases; however, the systems developed so far present several disadvantages. Here in this work, we report the development of genetically encoded dark-to-bright fluorescent reporter, activatable by the TBEV NS2B-NS3 protease for *in vitro* and in cell applications.

The construction and use of dark-to-bright fluorescence reporters have been previously reported for monitoring of caspase activity during apoptosis [64, 66, 67], the activity of NS2B-NS3 protease derived from DENV-2 and ZIKV [63], the activity of SARS-CoV-2 NS5 protease in inhibition assays [68], or activity of NS3 protease of classical swine fever virus [69]. All of the above mentioned studies have utilized either GFP or, in one case, mNeptune as fluorescence reporters. The introduction of fluorophores into living cells leads to the generation of reactive oxygen species (ROS) that cause damage to the cells. The amount of ROS generated by each fluorophore is different, and generally, the emission of green light causes higher phototoxicity than the emission of red light [70]. Even though GFP is a well-established fluorescence reporter in living systems, which can be easily detected without additional steps and manipulation with the sample, it still shows a rather high background. Therefore, we have designed a reporter using PAmCherry fluorescent protein. The advantage comes from the two-step activation, which is required for observation of fluorescence signal: (1) biological activation by NS2B-NS3 protease, (2) photoactivation with the light of 405 nm. This provides a system that is gentle to the cells in terms of ROS generation and high contrast over the background [71]. hMGFP reporter was designed for comparison of TBEV protease activity with an already established system for other flaviviral proteases as well as for *in vitro* studies.

For *in vitro* studies, both reporters were produced using various strains of competent *E. coli* cells, and production conditions. Despite the efforts, all production conditions showed accumulation of reporters in inclusion bodies, suggesting partial or improper folding of the produced reporters. This result is in contrast to the previously described reporters for caspase activation [64, 66] and for NS2B-NS3 protease from DENV-2 and ZIKV [63], where the reporters have been successfully produced using the same conditions as in this work - in BL21(DE3) competent *E. coli* cells using pET21b plasmid, 1 mM IPTG and temperature

20-25°C. Interestingly, production of the hMGFP lacking the cleavage site and quenching peptide showed, as expected, strong production in the soluble fraction, because hMGFP is codon-optimized for a high level of expression in *E. coli*. This suggests that the influenza M2 peptide interferes with the proper folding of the reporter. The influenza M2 protein is known to oligomerize into tetramers to form the ion channel by the formation of disulfide bridges between the two cysteine residues preceding the transmembrane region [72]. One of these cysteine residues (19-Cys) is present in the sequence of the quenching peptide. In addition, it was shown that the caspase activity reporter oligomerizes to tetramers and higher-order oligomers, which seems to prevent the formation of the chromophore [64]. This oligomerization could possibly be the reason for its presence in inclusion bodies.

As the majority of the reporter consists of the fluorescent protein, whose structural unit is a well-known β-barrel and should be relatively easy to fold [73], we purified both reporters under denaturing conditions and attempted to refold them into their native state by step-down refolding. While hMGFP reporter was present mainly in the precipitate, PAmCherry reporter was present in both soluble and insoluble fractions, but circular dichroism measurement was inconclusive due to possible contamination and high Tris concentration, and no recovery of fluorescence was observed upon incubation with TBEV NS2B-NS3pro. This suggests that the reporter did not possess the correct fold. Refolding by dialysis is a time-consuming, trial-and-error process, which often results in low protein recovery. However, the used procedure represents the basic refolding protocol, and the process can be further optimized and improved by the use of protein aggregation inhibitors such as polyethylene glycol, trehalose, or other additives that promote proper folding [74].

The pilot cleavage experiments of PAmCherry reporter with recombinant TBEV NS2B-NS3 protease showed two cleavage products. Performed MS analysis did not exactly identify the cleavage site for each product, likely due to the requirement for a protein of higher purity and the presence of no basic residues in the sequence of quenching peptide. As NS3 requires an NS2B cofactor for its proper function [36], covalent and non-covalent (unlinked) flaviviral protease constructs were reported in previous studies and displayed various activities towards the substrate [40, 45, 65, 75]. Therefore, the exact construct of the recombinant protease that was used in this work might affect the final activity and substrate specificity. In addition, protease concentrations used in the assay were relatively high thus promoting potential unspecific cleavage.

To evaluate the efficiency of both reporters to monitor TBEV NS2B-NS3 protease activity in living cells, stably transduced Vero E6 and BHK-21 cells were infected with TBEV. Even though quantitation of fluorescence was possible only for the PAmCherry signal, comparison of images of PAmCherry signal (Figure 26 and 27) with the hMGFP signal (Figure 30 and 31) in cells clearly shows a significant difference for background fluorescence. While there is a minimum background for the PAmCherry in the non-photoactivated state, hMGFP shows high levels of fluorescence in the control samples not treated with TBEV, which makes it difficult to evaluate the effect of infection. This background, markedly higher in Vero E6 likely results from cleavage of the reporter by cellular proteases which share the same specificity for two consecutive arginine residues. PAmCherry background consists of a signal localized in confined vesicles, where the change in pH may lead to the activation of the PAmCherry. Mechanism of activation of PAmCherry consists in excitation of the chromophore with 405 nm, which leads to the formation of radicals that abstract a proton from Tyr-67 C^{β}. This results in the formation of C^{α}-C^{β}double bond in Tyr-67 and conjugation of two aromatic rings thus shifting the absorbance from 405 nm to 564 nm [76]. Quantitative analysis of PAmCherry signal showed an increase in SBR throughout infection to ~ 2-3, which is a similar level of increase that was observed for GFP-based reporters of protease activity of DENV-2 and considerably higher than observed for ZIKV protease [63]. Although PAmCherry shows promising potential for monitoring protease activity in living cells with significantly lower background, long lifetimes, and brightness, the method needs to be optimized for further applications.

6 Conclusions

In this thesis, we have designed and produced two cleavage reporters (PAmCherry and hMGFP) for monitoring TBEV NS2B-NS3 protease activity. Despite using several *E. coli* strains, neither of the reporters was produced in the soluble form. The attempted denaturing purification followed by refolding did not yield any correctly folded reporter, therefore further optimization of expression conditions is necessary to obtain the reporter in the soluble fraction for *in vitro* experiments. Successful production of the properly folded reporter could provide a simple but precise and valuable tool for in vitro testing of recombinant TBEV NS2B-NS3 protease activity, its mutants, and potential protease inhibitors.

Live cell imaging showed a correlation between the activity of the NS2B-NS3 protease and an increase in fluorescence over the time of infection. In the case of PAmCherry, the SBR increased to 2-3 over the course of infection as well as localization of the fluorescence signal changed from confined vesicles to the whole volume of the cytoplasm. Compared to the hMGFP reporter, the PAmCherry reporter provides significantly lower background and higher stability upon photobleaching. Vero E6 cell line seems to be more suitable for live imaging due to lower virus-induced cytotoxicity, but usage of lower virulence TBEV strain (eg. Neudörfl) could provide further insights and possibly a longer observation period. In the future, the method might as well benefit from the use of single clone stable cell lines expressing the reporter, instead of a polyclonal stable cell line, as a way to reduce the differences in fluorescence between individual cells due to the different levels of expression of the reporter. Even though the PAmCherry reporter shows to be a promising tool for monitoring the protease activity with high sensitivity and low background, this method needs to be further optimized and more measurements performed to obtain more precise data and lower standard deviations between individual observations.

7 References

1 Gould, E. A. & Solomon, T. (2008). Pathogenic flaviviruses. The Lancet, 371, 500–509. 10.1016/S0140-6736(08)60238-X.

2 Barrows, N. J., Campos, R. K., Liao, K.-C., Prasanth, K. R., Soto-Acosta, R., Yeh, S.-C., Schott-Lerner, G., Pompon, J., Sessions, O. M., Bradrick, S. S. & Garcia-Blanco, M. A. (2018). Biochemistry and Molecular Biology of Flaviviruses. Chemical reviews, 118, 4448–4482. 10.1021/acs.chemrev.7b00719.

3 Blitvich, B. J. & Firth, A. E. (2017). A Review of Flaviviruses that Have No Known Arthropod Vector. Viruses, 9. 10.3390/v9060154.

4 Goh, V. S. L., Mok, C.-K. & Chu, J. J. H. (2020). Antiviral Natural Products for Arbovirus Infections. Molecules (Basel, Switzerland), 25. 10.3390/molecules25122796.

5 Ruzek, D., Avšič Županc, T., Borde, J., Chrdle, A., Eyer, L., Karganova, G., Kholodilov, I., Knap, N., Kozlovskaya, L., Matveev, A., Miller, A. D., Osolodkin, D. I., Överby, A. K., Tikunova, N., Tkachev, S. & Zajkowska, J. (2019). Tick-borne encephalitis in Europe and Russia: Review of pathogenesis, clinical features, therapy, and vaccines. Antiviral research, 164, 23–51. 10.1016/j.antiviral.2019.01.014.

6 Pulkkinen, L. I. A., Butcher, S. J. & Anastasina, M. (2018). Tick-Borne Encephalitis Virus: A Structural View. Viruses, 10. 10.3390/v10070350.

7 Ecker, M., Allison, S. L., Meixner, T. & Heinz, F. X. (1999). Sequence analysis and genetic classification of tick-borne encephalitis viruses from Europe and Asia. The Journal of general virology, 80 (Pt 1), 179–185. 10.1099/0022-1317-80-1-179.

8 Gritsun, T. S., Frolova, T. V., Zhankov, A. I., Armesto, M., Turner, S. L., Frolova, M. P., Pogodina, V. V., Lashkevich, V. A. & Gould, E. A. (2003). Characterization of a siberian virus isolated from a patient with progressive chronic tick-borne encephalitis. Journal of virology, 77, 25–36. 10.1128/JVI.77.1.25-36.2003.

9 Kríz, B., Benes, C. & Daniel, M. (2009). Alimentary transmission of tick-borne encephalitis in the Czech Republic (1997-2008). Epidemiologie, mikrobiologie, imunologie: casopis Spolecnosti pro epidemiologii a mikrobiologii Ceske lekarske spolecnosti J.E. Purkyne, 58, 98–103,

10 Mansfield, K. L., Johnson, N., Phipps, L. P., Stephenson, J. R., Fooks, A. R. & Solomon, T. (2009). Tick-borne encephalitis virus - a review of an emerging zoonosis. The Journal of general virology, 90, 1781–1794. 10.1099/vir.0.011437-0.

11 Chimitia-Dobler, L. (2020). Chapter 3: Transmission/ Natural Cycle. Tick-borne encephalitis - The Book. 10.33442/26613980_3-3.

12 Labuda, M., Jones, L. D., Williams, T. & Nuttall, P. A. (1993). Enhancement of tick-borne encephalitis virus transmission by tick salivary gland extracts. Medical and veterinary entomology, 7, 193–196. 10.1111/j.1365-2915.1993.tb00674.x.

13 Labuda, M., Austyn, J. M., Zuffova, E., Kozuch, O., Fuchsberger, N., Lysy, J. & Nuttall, P. A. (1996). Importance of localized skin infection in tick-borne encephalitis virus transmission. Virology, 219, 357–366. 10.1006/viro.1996.0261.

14 Růžek, D., Salát, J., Singh, S. K. & Kopecký, J. (2011). Breakdown of the blood-brain barrier during tick-borne encephalitis in mice is not dependent on CD8+ T-cells. PloS one, 6, e20472. 10.1371/journal.pone.0020472.

15 Füzik, T., Formanová, P., Růžek, D., Yoshii, K., Niedrig, M. & Plevka, P. (2018). Structure of tick-borne encephalitis virus and its neutralization by a monoclonal antibody. Nature communications, 9, 436. 10.1038/s41467-018-02882-0.

16 Zhang, Y., Kostyuchenko, V. A. & Rossmann, M. G. (2007). Structural analysis of viral nucleocapsids by subtraction of partial projections. Journal of structural biology, 157, 356–364. 10.1016/j.jsb.2006.09.002.

17 Rey, F. A., Heinz, F. X., Mandl, C., Kunz, C. & Harrison, S. C. (1995). The envelope glycoprotein from tick-borne encephalitis virus at 2 A resolution. Nature, 375, 291–298. 10.1038/375291a0.

18 Goto, A., Yoshii, K., Obara, M., Ueki, T., Mizutani, T., Kariwa, H. & Takashima, I. (2005). Role of the N-linked glycans of the prM and E envelope proteins in tick-borne encephalitis virus particle secretion. Vaccine, 23, 3043–3052. 10.1016/j.vaccine.2004.11.068.

19 Yoshii, K., Yanagihara, N., Ishizuka, M., Sakai, M. & Kariwa, H. (2013). N-linked glycan in tick-borne encephalitis virus envelope protein affects viral secretion in mammalian cells, but not in tick cells. The Journal of general virology, 94, 2249–2258. 10.1099/vir.0.055269-0.

20 Barnard, T. R., Abram, Q. H., Lin, Q. F., Wang, A. B. & Sagan, S. M. (2021). Molecular Determinants of Flavivirus Virion Assembly. Trends in biochemical sciences, 46, 378–390. 10.1016/j.tibs.2020.12.007.

21 Malygin, A. A., Bondarenko, E. I., Ivanisenko, V. A., Protopopova, E. V., Karpova, G. G. & Loktev, V. B. (2009). C-terminal fragment of human laminin-binding protein contains a receptor domain for venezuelan equine encephalitis and tick-borne encephalitis viruses. Biochemistry. Biokhimiia, 74, 1328–1336. 10.1134/s0006297909120050.

22 Zaitsev, B. N., Benedetti, F., Mikhaylov, A. G., Korneev, D. V., Sekatskii, S. K., Karakouz, T., Belavin, P. A., Netesova, N. A., Protopopova, E. V., Konovalova, S. N., Dietler, G. & Loktev, V. B. (2014). Force-induced globule-coil transition in laminin binding protein and its role for viral-cell membrane fusion. Journal of molecular recognition : JMR, 27, 727–738. 10.1002/jmr.2399.

23 Kroschewski, H., Allison, S. L., Heinz, F. X. & Mandl, C. W. (2003). Role of heparan sulfate for attachment and entry of tick-borne encephalitis virus. Virology, 308, 92–100. 10.1016/S0042-6822(02)00097-1.

24 Rodrigues, R., Danskog, K., Överby, A. K. & Arnberg, N. (2019). Characterizing the cellular attachment receptor for Langat virus. PloS one, 14, e0217359. 10.1371/journal.pone.0217359.

25 Phillpotts, R. J., Stephenson, J. R. & Porterfield, J. S. (1985). Antibody-dependent enhancement of tick-borne encephalitis virus infectivity. The Journal of general virology, 66 (Pt 8), 1831–1837. 10.1099/0022-1317-66-8-1831.

26 Heinz, F. X. & Allison, S. L. (2003). Flavivirus Structure and Membrane Fusion. Elsevier, 63–97. ISBN 9780120398591.

27 Tan, T. Y., Fibriansah, G., Kostyuchenko, V. A., Ng, T.-S., Lim, X.-X., Zhang, S., Lim, X.-N., Wang, J., Shi, J., Morais, M. C., Corti, D. & Lok, S.-M. (2020). Capsid protein structure in Zika virus reveals the flavivirus assembly process. Nature communications, 11, 895. 10.1038/s41467-020-14647-9.

28 Shang, Z., Song, H., Shi, Y., Qi, J. & Gao, G. F. (2018). Crystal Structure of the Capsid Protein from Zika Virus. Journal of molecular biology, 430, 948–962. 10.1016/j.jmb.2018.02.006.

29 López, C., Gil, L., Lazo, L., Menéndez, I., Marcos, E., Sánchez, J., Valdés, I., Falcón, V., La Rosa, M. C. de, Márquez, G., Guillén, G. & Hermida, L. (2009). In vitro assembly of nucleocapsid-like particles from purified recombinant capsid protein of dengue-2 virus. Archives of virology, 154, 695–698. 10.1007/s00705-009-0350-8.

30 Xie, X., Zou, J., Zhang, X., Zhou, Y., Routh, A. L., Kang, C., Popov, V. L., Chen, X., Wang, Q.-Y., Dong, H. & Shi, P.-Y. (2019). Dengue NS2A Protein Orchestrates Virus Assembly. Cell host & microbe, 26, 606-622.e8. 10.1016/j.chom.2019.09.015.

31 Zhang, X., Xie, X., Xia, H., Zou, J., Huang, L., Popov, V. L., Chen, X. & Shi, P.-Y. (2019). Zika Virus NS2A-Mediated Virion Assembly. mBio, 10. 10.1128/mBio.02375-19.

32 Kostyuchenko, V. A., Zhang, Q., Tan, J. L., Ng, T.-S. & Lok, S.-M. (2013). Immature and mature dengue serotype 1 virus structures provide insight into the maturation process. Journal of virology, 87, 7700–7707. 10.1128/JVI.00197-13.

33 Chambers, T. J., Weir, R. C., Grakoui, A., McCourt, D. W., Bazan, J. F., Fletterick, R. J. & Rice, C. M. (1990). Evidence that the N-terminal domain of nonstructural protein NS3 from yellow fever virus is a serine protease responsible for site-specific cleavages in the viral polyprotein. Proceedings of the National Academy of Sciences of the United States of America, 87, 8898–8902. 10.1073/pnas.87.22.8898.

34 Luo, D., Vasudevan, S. G. & Lescar, J. (2015). The flavivirus NS2B-NS3 protease-helicase as a target for antiviral drug development. Antiviral research, 118, 148–158. 10.1016/j.antiviral.2015.03.014.

35 Aleshin, A. E., Shiryaev, S. A., Strongin, A. Y. & Liddington, R. C. (2007). Structural evidence for regulation and specificity of flaviviral proteases and evolution of the Flaviviridae fold. Protein science: a publication of the Protein Society, 16, 795–806. 10.1110/ps.072753207.

36 Clum, S., Ebner, K. E. & Padmanabhan, R. (1997). Cotranslational membrane insertion of the serine proteinase precursor NS2B-NS3(Pro) of dengue virus type 2 is required for efficient in vitro processing and is mediated through the hydrophobic regions of NS2B. The Journal of biological chemistry, 272, 30715–30723. 10.1074/jbc.272.49.30715.

37 Robin, G., Chappell, K., Stoermer, M. J., Hu, S.-H., Young, P. R., Fairlie, D. P. & Martin, J. L. (2009). Structure of West Nile virus NS3 protease: ligand stabilization of the

catalytic conformation. Journal of molecular biology, 385, 1568–1577. 10.1016/j.jmb.2008.11.026.

38 Erbel, P., Schiering, N., D'Arcy, A., Renatus, M., Kroemer, M., Lim, S. P., Yin, Z., Keller, T. H., Vasudevan, S. G. & Hommel, U. (2006). Structural basis for the activation of flaviviral NS3 proteases from dengue and West Nile virus. Nature structural & molecular biology, 13, 372–373. 10.1038/nsmb1073.

39 Chandramouli, S., Joseph, J. S., Daudenarde, S., Gatchalian, J., Cornillez-Ty, C. & Kuhn, P. (2010). Serotype-specific structural differences in the protease-cofactor complexes of the dengue virus family. Journal of virology, 84, 3059–3067. 10.1128/JVI.02044-09.

40 Lei, J., Hansen, G., Nitsche, C., Klein, C. D., Zhang, L. & Hilgenfeld, R. (2016). Crystal structure of Zika virus NS2B-NS3 protease in complex with a boronate inhibitor. Science (New York, N.Y.), 353, 503–505. 10.1126/science.aag2419.

41 Chambers, T. J., Nestorowicz, A., Amberg, S. M. & Rice, C. M. (1993). Mutagenesis of the yellow fever virus NS2B protein: effects on proteolytic processing, NS2B-NS3 complex formation, and viral replication. Journal of virology, 67, 6797–6807. 10.1128/JVI.67.11.6797-6807.1993.

42 Menéndez-Arias, L. (2010). Molecular basis of human immunodeficiency virus drug resistance: an update. Antiviral research, 85, 210–231. 10.1016/j.antiviral.2009.07.006.

43 Li, Z., Zhang, J. & Li, H. (2017). Flavivirus NS2B/NS3 Protease: Structure, Function, and Inhibition. Elsevier, 163–188. ISBN 9780128097120.

44 Potapova, U. V., Feranchuk, S. I., Potapov, V. V., Kulakova, N. V., Kondratov, I. G., Leonova, G. N. & Belikov, S. I. (2012). NS2B/NS3 protease: allosteric effect of mutations associated with the pathogenicity of tick-borne encephalitis virus. Journal of biomolecular structure & dynamics, 30, 638–651. 10.1080/07391102.2012.689697.

45 Leung, D., Schroder, K., White, H., Fang, N. X., Stoermer, M. J., Abbenante, G., Martin, J. L., Young, P. R. & Fairlie, D. P. (2001). Activity of recombinant dengue 2 virus NS3 protease in the presence of a truncated NS2B co-factor, small peptide substrates, and inhibitors. The Journal of biological chemistry, 276, 45762–45771. 10.1074/jbc.M107360200.

46 Li, J., Lim, S. P., Beer, D., Patel, V., Wen, D., Tumanut, C., Tully, D. C., Williams, J. A., Jiricek, J., Priestle, J. P., Harris, J. L. & Vasudevan, S. G. (2005). Functional profiling of

recombinant NS3 proteases from all four serotypes of dengue virus using tetrapeptide and octapeptide substrate libraries. The Journal of biological chemistry, 280, 28766–28774. 10.1074/jbc.M500588200.

47 Mangano, D. T., Miao, Y., Vuylsteke, A., Tudor, I. C., Juneja, R., Filipescu, D., Hoeft, A., Fontes, M. L., Hillel, Z., Ott, E., Titov, T., Dietzel, C. & Levin, J. (2007). Mortality associated with aprotinin during 5 years following coronary artery bypass graft surgery. JAMA, 297, 471–479. 10.1001/jama.297.5.471.

48 Mangano, D. T., Tudor, I. C. & Dietzel, C. (2006). The risk associated with aprotinin in cardiac surgery. The New England journal of medicine, 354, 353–365. 10.1056/NEJMoa051379.

49 Rothan, H. A., Han, H. C., Ramasamy, T. S., Othman, S., Rahman, N. A. & Yusof, R. (2012). Inhibition of dengue NS2B-NS3 protease and viral replication in Vero cells by recombinant retrocyclin-1. BMC infectious diseases, 12, 314. 10.1186/1471-2334-12-314.

50 Tomlinson, S. M., Malmstrom, R. D., Russo, A., Mueller, N., Pang, Y.-P. & Watowich, S. J. (2009). Structure-based discovery of dengue virus protease inhibitors. Antiviral research, 82, 110–114. 10.1016/j.antiviral.2009.02.190.

51 Tomlinson, S. M. & Watowich, S. J. (2011). Anthracene-based inhibitors of dengue virus NS2B-NS3 protease. Antiviral research, 89, 127–135. 10.1016/j.antiviral.2010.12.006.

52 Yang, C.-C., Hsieh, Y.-C., Lee, S.-J., Wu, S.-H., Liao, C.-L., Tsao, C.-H., Chao, Y.-S., Chern, J.-H., Wu, C.-P. & Yueh, A. (2011). Novel dengue virus-specific NS2B/NS3 protease inhibitor, BP2109, discovered by a high-throughput screening assay. Antimicrobial agents and chemotherapy, 55, 229–238. 10.1128/AAC.00855-10.

53 Mueller, N. H., Pattabiraman, N., Ansarah-Sobrinho, C., Viswanathan, P., Pierson, T. C. & Padmanabhan, R. (2008). Identification and biochemical characterization of small-molecule inhibitors of west nile virus serine protease by a high-throughput screen. Antimicrobial agents and chemotherapy, 52, 3385–3393. 10.1128/AAC.01508-07.

54 Pambudi, S., Kawashita, N., Phanthanawiboon, S., Omokoko, M. D., Masrinoul, P., Yamashita, A., Limkittikul, K., Yasunaga, T., Takagi, T., Ikuta, K. & Kurosu, T. (2013). A small compound targeting the interaction between nonstructural proteins 2B and 3 inhibits dengue virus replication. Biochemical and biophysical research communications, 440, 393–398. 10.1016/j.bbrc.2013.09.078.

55 Akaberi, D., Båhlström, A., Chinthakindi, P. K., Nyman, T., Sandström, A., Järhult, J. D., Palanisamy, N., Lundkvist, Å. & Lennerstrand, J. (2021). Targeting the NS2B-NS3 protease of tick-borne encephalitis virus with pan-flaviviral protease inhibitors. Antiviral research, 190, 105074. 10.1016/j.antiviral.2021.105074.

56 Balsitis, S. J., Coloma, J., Castro, G., Alava, A., Flores, D., McKerrow, J. H., Beatty, P. R. & Harris, E. (2009). Tropism of dengue virus in mice and humans defined by viral nonstructural protein 3-specific immunostaining. The American journal of tropical medicine and hygiene, 80, 416–424,

57 Tamura, T., Fukuhara, T., Uchida, T., Ono, C., Mori, H., Sato, A., Fauzyah, Y., Okamoto, T., Kurosu, T., Setoh, Y. X., Imamura, M., Tautz, N., Sakoda, Y., Khromykh, A. A., Chayama, K. & Matsuura, Y. (2018). Characterization of Recombinant Flaviviridae Viruses Possessing a Small Reporter Tag. Journal of virology, 92. 10.1128/JVI.01582-17.

58 Li, S.-H., Li, X.-F., Zhao, H., Deng, Y.-Q., Yu, X.-D., Zhu, S.-Y., Jiang, T., Ye, Q., Qin, E.-D. & Qin, C.-F. (2013). Development and characterization of the replicon system of Japanese encephalitis live vaccine virus SA14-14-2. Virology journal, 10, 64. 10.1186/1743-422X-10-64.

59 Xie, X., Zou, J., Shan, C., Yang, Y., Kum, D. B., Dallmeier, K., Neyts, J. & Shi, P.-Y. (2016). Zika Virus Replicons for Drug Discovery. EBioMedicine, 12, 156–160. 10.1016/j.ebiom.2016.09.013.

60 Kümmerer, B. M. (2018). Establishment and Application of Flavivirus Replicons. Advances in experimental medicine and biology, 1062, 165–173. 10.1007/978-981-10-8727-1_12.

61 McFadden, M. J., Mitchell-Dick, A., Vazquez, C., Roder, A. E., Labagnara, K. F., McMahon, J. J., Silver, D. L. & Horner, S. M. (2018). A Fluorescent Cell-Based System for Imaging Zika Virus Infection in Real-Time. Viruses, 10. 10.3390/v10020095.

62 Medin, C. L., Valois, S., Patkar, C. G. & Rothman, A. L. (2015). A plasmid-based reporter system for live cell imaging of dengue virus infected cells. Journal of virological methods, 211, 55–62. 10.1016/j.jviromet.2014.10.010.

63 Arias-Arias, J. L., MacPherson, D. J., Hill, M. E., Hardy, J. A. & Mora-Rodríguez, R. (2020). A fluorescence-activatable reporter of flavivirus NS2B-NS3 protease activity enables

live imaging of infection in single cells and viral plaques. The Journal of biological chemistry, 295, 2212–2226. 10.1074/jbc.RA119.011319.

64 Nicholls, S. B. & Hardy, J. A. (2013). Structural basis of fluorescence quenching in caspase activatable-GFP. Protein science : a publication of the Protein Society, 22, 247–257. 10.1002/pro.2188.

65 Vejvodová, K. (2021). Recombinant production and characterization of protease domain from TBEV nonstructural protein NS3, Faculty of Science, University of South Bohemia in České Budějovice.

66 Nicholls, S. B., Chu, J., Abbruzzese, G., Tremblay, K. D. & Hardy, J. A. (2011). Mechanism of a genetically encoded dark-to-bright reporter for caspase activity. The Journal of biological chemistry, 286, 24977–24986. 10.1074/jbc.M111.221648.

67 Wu, P., Nicholls, S. B. & Hardy, J. A. (2013). A tunable, modular approach to fluorescent protease-activated reporters. Biophysical journal, 104, 1605–1614. 10.1016/j.bpj.2013.01.058.

68 Mahdi, M., Mótyán, J. A., Szojka, Z. I., Golda, M., Miczi, M. & Tőzsér, J. (2020). Analysis of the efficacy of HIV protease inhibitors against SARS-CoV-2's main protease. Virology journal, 17, 190. 10.1186/s12985-020-01457-0.

69 Chen, F., Yang, X., Pang, D., Peng, Z., Ma, T., Ouyang, H. & Ren, L. (2015). A dark-to-bright reporter cell for classical swine fever virus infection. Antiviral research, 117, 44–51. 10.1016/j.antiviral.2015.02.009.

70 Icha, J., Weber, M., Waters, J. C. & Norden, C. (2017). Phototoxicity in live fluorescence microscopy, and how to avoid it. BioEssays: news and reviews in molecular, cellular and developmental biology, 39. 10.1002/bies.201700003.

71 Subach, F. V., Patterson, G. H., Manley, S., Gillette, J. M., Lippincott-Schwartz, J. & Verkhusha, V. V. (2009). Photoactivatable mCherry for high-resolution two-color fluorescence microscopy. Nature methods, 6, 153–159. 10.1038/nmeth.1298.

72 Sugrue, R. J. & Hay, A. J. (1991). Structural characteristics of the M2 protein of influenza a viruses: Evidence that it forms a tetrameric channel. Virology, 180, 617–624. 10.1016/0042-6822(91)90075-M.

73 Enoki, S., Saeki, K., Maki, K. & Kuwajima, K. (2004). Acid denaturation and refolding of green fluorescent protein. Biochemistry, 43, 14238–14248. 10.1021/bi048733+.

74 Yamaguchi, H. & Miyazaki, M. (2014). Refolding techniques for recovering biologically active recombinant proteins from inclusion bodies. Biomolecules, 4, 235–251. 10.3390/biom4010235.

75 Kuiper, B. D., Slater, K., Spellmon, N., Holcomb, J., Medapureddy, P., Muzzarelli, K. M., Yang, Z., Ovadia, R., Amblard, F., Kovari, I. A., Schinazi, R. F. & Kovari, L. C. (2017). Increased activity of unlinked Zika virus NS2B/NS3 protease compared to linked Zika virus protease. Biochemical and biophysical research communications, 492, 668–673. 10.1016/j.bbrc.2017.03.108.

76 Subach, F. V., Malashkevich, V. N., Zencheck, W. D., Xiao, H., Filonov, G. S., Almo, S. C. & Verkhusha, V. V. (2009). Photoactivation mechanism of PAmCherry based on crystal structures of the protein in the dark and fluorescent states. Proceedings of the National Academy of Sciences of the United States of America, 106, 21097–21102. 10.1073/pnas.0909204106.

8 Supplements

8.1 Cleavage reporter sequences

8.1.1 PAmCherry reporter

DNA sequence:

ATGGTGAGCAAGGGCGAGGAGGATAACATGGCCATCATTAAGGAGTTCATGCG
CTTCAAGGTGCACATGGAGGGGTCCGTGAACGGCCACGTGTTCGAGATCGAGGG
CGAGGGCGAGGGCCGCCCCTACGAGGGCACCCAGACCGCCAAGCTGAAGGTGA
CCAAGGGCGGCCCCCTGCCCTTCACCTGGGACATCCTGAGCCCTCAGTTCATGTA
CGGCTCCAATGCCTACGTGAAGCACCCCGCCGACATCCCCGACTACTTTAAGCT
GTCCTTCCCCGAGGGCTTCAAGTGGGAGCGCGTGATGAAATTCGAGGACGGCGG
CGTGGTGACCGTGACCCAGGACTCCTCCCTGCAGGACGGCGAGTTCATCTACAA
GGTGAAGCTGCGCGGCACCAACTTCCCCTCCGACGGCCCCGTGATGCAGAAGAA
GACCATGGGCTGGGAGGCCCTCTCCGAGCGGATGTACCCCGAGGACGGCGCCCT
GAAGGGCGAGGTCAAGCCCAGAGTGAAGCTGAAGGACGGCGGCCACTACGACG
CTGAGGTCAAGACCACCTACAAGGCCAAGAAGCCCGTGCAGCTGCCCGGCGCCT
ACAACGTCAACCGCAAGCTGGACATCACCAGCCACAACGAGGACTACACCATC
GTGGAGCAGTACGAGAGAGCCGAGGGCCGCCACTCCACCGGCGGCATGGACGA
GCTGTACAAG**GCTGCCCAACGGCGCGGAAGAGTTGGT**TGCAACGATTCAAGT
GACCCGCTTGTTGTTGCTGCGAGTATCATTGGGATCTTGCACTTGATATTGTGGA
TTCTTGATCGTCTTTAA

Note: TBEV NS2B-NS3 cleavage site is highlighted in bold, while the inhibition peptide sequence is underlined.

Protein sequence:

MVSKGEEDNMAIIKEFMRFKVHMEGSVNGHVFEIEGEGEGRPYEGTQTAKLKVTK
GGPLPFTWDILSPQFMYGSNAYVKHPADIPDYFKLSFPEGFKWERVMKFEDGGVVT
VTQDSSLQDGEFIYKVKLRGTNFPSDGPVMQKKTMGWEALSERMYPEDGALKGEV
KPRVKLKDGGHYDAEVKTTYKAKKPVQLPGAYNVNRKLDITSHNEDYTIVEQYER
AEGRHSTGGMDELYKAAQRRGRVGCNDSSDPLVVAASIIGILHLILWILDRL-

Number of amino acids: 273

Molecular weight: 30.761 kDa

Theoretical pI: 6.20

Molar extinction coefficient: 39880 $M^{-1}cm^{-1}$

8.1.2 hMGFP reporter

DNA sequence:

ATGGGCGTGATCAAGCCCGACATGAAGATCAAGCTGCGGATGGAGGGCGCCGT
GAACGGCCACAAATTCGTGATCGAGGGCGACGGGAAAGGCAAGCCCTTTGAGG
GTAAGCAGACTATGGACCTGACCGTGATCGAGGGCGCCCCCCTGCCCTTCGCTT
ATGACATTCTCACCACCGTGTTCGACTACGGTAACCGTGTCTTCGCCAAGTACCC
CAAGGACATCCCTGACTACTTCAAGCAGACCTTCCCCGAGGGCTACTCGTGGGA
GCGAAGCATGACATACGAGGACCAGGGAATCTGTATCGCTACAAACGACATCA
CCATGATGAAGGGTGTGGACGACTGCTTCGTGTACAAAATCCGCTTCGACGGGG
TCAACTTCCCTGCTAATGGCCCGGTGATGCAGCGCAAGACCCTAAAGTGGGAGC
CCAGTACCGAGAAGATGTACGTGCGGGACGGCGTACTGAAGGGCGATGTTAAT
ATGGCACTGCTCTTGGAGGGAGGCGGCCACTACCGCTGCGACTTCAAGACCACC
TACAAAGCCAAGAAGGTGGTGCAGCTTCCCGACTACCACTTCGTGGACCACCGC
ATCGAGATCGTGAGCCACGACAAGGACTACAACAAAGTCAAGCTGTACGAGCA
CGCCGAAGCCCACAGCGGACTACCCCGCCAGGCCGGC**GCTGCCCAACGGCGC**
GGAAGAGTTGGTTGCAACGATTCAAGTGACCCGCTTGTTGTTGCTGCGAGTATC
ATTGGGATCTTGCACTTGATATTGTGGATTCTTGATCGTCTTTAA

Note: TBEV NS2B-NS3 cleavage site is highlighted in bold, while the inhibition peptide sequence is underlined.

Protein sequence:

MGVIKPDMKIKLRMEGAVNGHKFVIEGDGKGKPFEGKQTMDLTVIEGAPLPFAYDI
LTTVFDYGNRVFAKYPKDIPDYFKQTFPEGYSWERSMTYEDQGICIATNDITMMKG
VDDCFVYKIRFDGVNFPANGPVMQRKTLKWEPSTEKMYVRDGVLKGDVNMALLL
EGGGHYRCDFKTTYKAKKVVQLPDYHFVDHRIEIVSHDKDYNKVKLYEHAEAHSG
LPRQAGAAQRRGRVGCNDSSDPLVVAASIIGILHLILWILDRL-

Number of amino acids: 264

Molecular weight: 29.934 kDa

Theoretical pI: 7.67

Molar extinction coefficient: 36120 $M^{-1}cm^{-1}$

8.2 Results

8.2.1 Pilot expression of PAmCherry reporter using pET19b

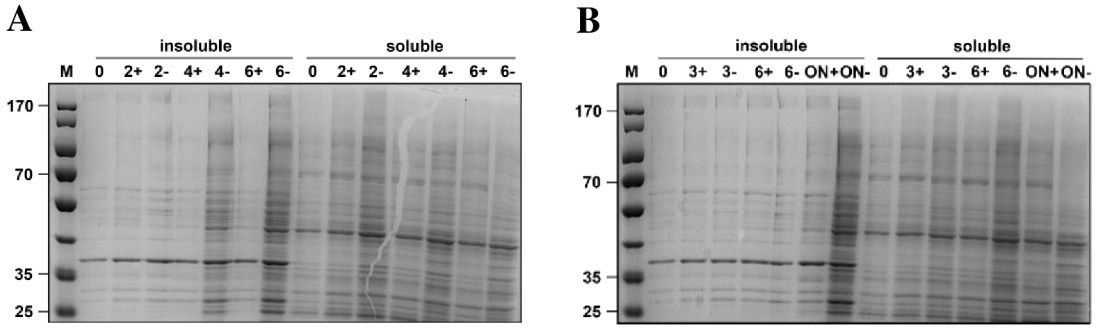

Figure 32 – **SDS-PAGE analysis of PAmCherry reporter expression in pET19b in BL21-CodonPlus cells.** A – 30°C, B – 18°C. M – PageRuler Prestained Protein Ladder (Thermo Fischer). – sign indicates uninduced culture, + sign indicates induced culture**,** each number represents an hour of collection of the sample after the induction.

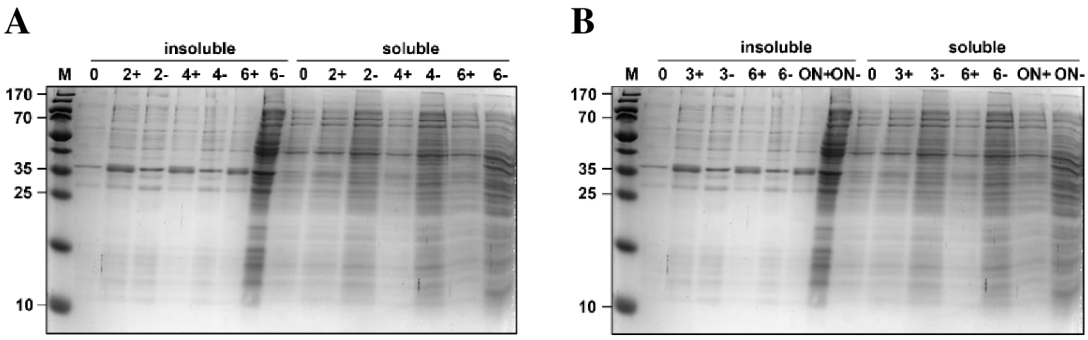

Figure 33 – **SDS-PAGE analysis of PAmCherry reporter expression in pET19b in BL21(DE3) cells.** A – 30°C, B – 18°C. M – PageRuler Prestained Protein Ladder (Thermo Fischer). – sign indicates uninduced culture, + sign indicates induced culture**,** each number represents an hour of collection of the sample after the induction.

8.2.2 Pilot expression of hMGFP reporter in One Shot® BL21(DE3)pLysS and Rosetta-gami® 2(DE3)

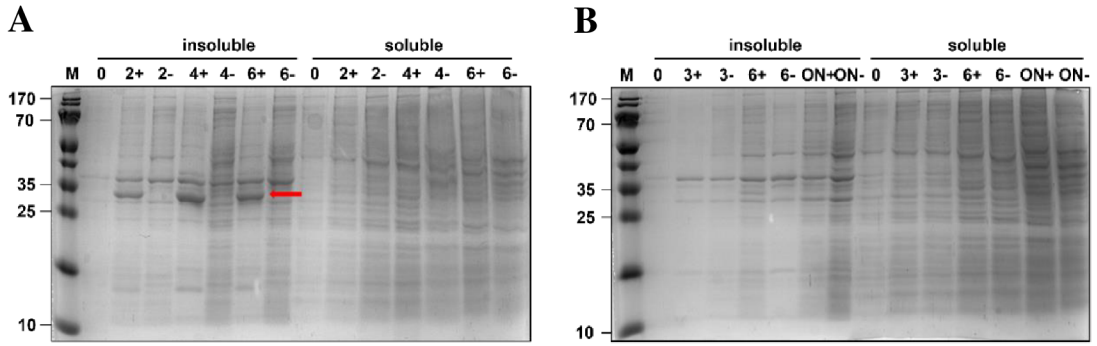

Figure 34 – **SDS-PAGE analysis of hMGFP reporter expression in One Shot® BL21(DE3)pLysS cells.** A – 30°C, B – 18°C. M – PageRuler Prestained Protein Ladder (Thermo Fischer). – sign indicates uninduced culture, + sign indicates induced culture**,** each number represents an hour of collection of the sample after the induction.

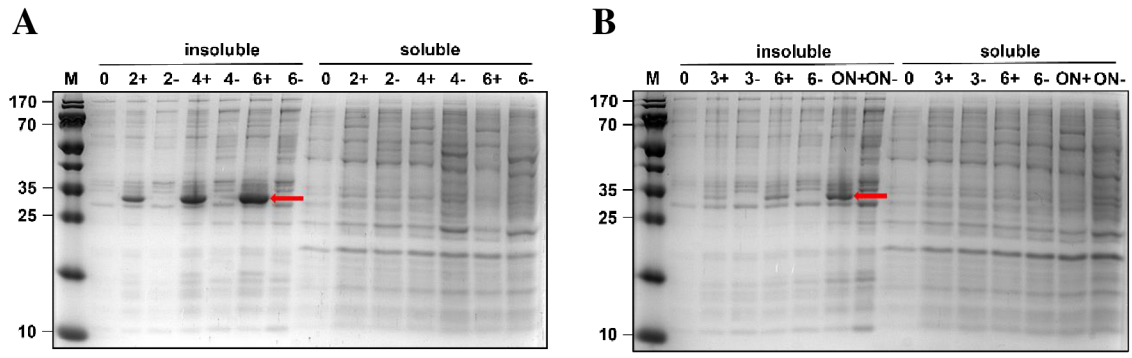

Figure 35 – **SDS-PAGE analysis of hMGFP reporter expression in Rosetta-gami® 2(DE3) cells.** A – 30°C, B – 18°C. M – PageRuler Prestained Protein Ladder (Thermo Fischer). – sign indicates uninduced culture, + sign indicates induced culture**,** each number represents an hour of collection of the sample after the induction.

8.2.3 Native purification of hMGFP reporter using HisTrap™ HP column

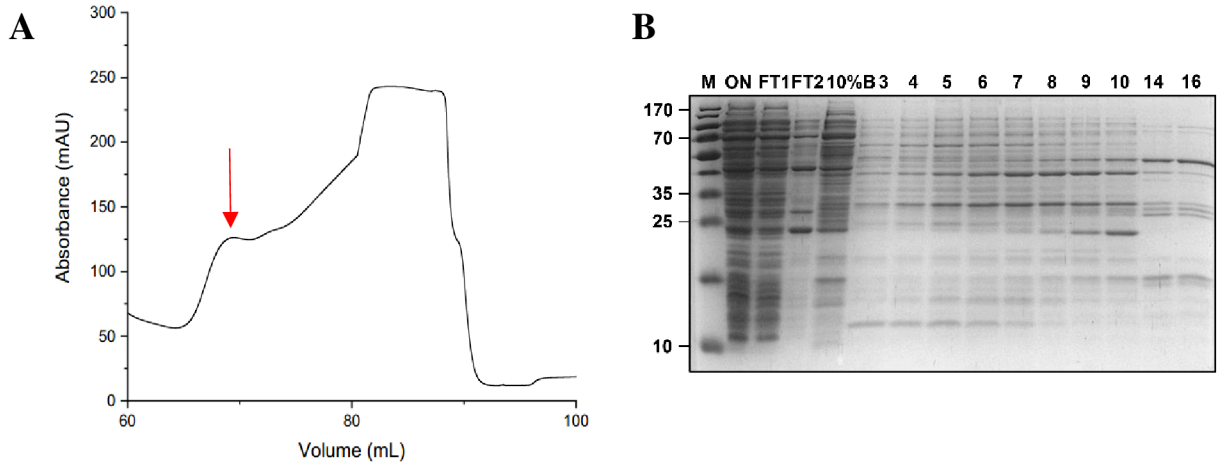

Figure 36 – **Native purification of hMGFP reporter.** A – Purification chromatogram. B – SDS-PAGE analysis of IMAC purification. M – PageRuler Restrained Protein Ladder (Thermo Fischer). ON – sample loaded onto the column, FT1 – flow-through fraction 1, FT2 – flow-through fraction 2, 10% B – eluate with 10% elution buffer, 3 – 16 eluted fractions with hMGFP reporter.

8.2.4 Mass spectrometry analysis of PAmCherry reporter cleavage products

Three cleavage products from time point 1.5h and concentration of NS2B-NS3 protease of 4 μM were cut out from the gel and each of them was analyzed by mass spectrometry (performed by Mgr. Filip Dyčka, Ph.D.) to identify where the cleavage occurred. Red colour marks the peptides captured during the analysis, black colour represents peptides that were not observed.

A – top protein band – presumably uncut reporter

MVSKGEEDNMAIIKEFMRFKVHMEGSVNGHVFEIEGEGEGRPYEGTQTAKLKVTKGGPLPF
TWDILSPQFMYGSNAYVKHPADIPDYFKLSFPEGFKWERVMKFEDGGVVTVTQDSSLQDGE
FIYKVKLRGTNFPSDGPVMQKKTMGWEALSERMYPEDGALKGEVKPRVKLKDGGHYDAE
VKTTYKAKKPVQLPGAYNVNRKLDITSHNEDYTIVEQYERAEGRHSTGGMDELYKAAQRR
GRVGCNDSSDPLVVAASIIGILHLILWILDRL

B – middle protein band

MVSKGEEDNMAIIKEFMRFKVHMEGSVNGHVFEIEGEGEGRPYEGTQTAKLKVTKGGPLPF
TWDILSPQFMYGSNAYVKHPADIPDYFKLSFPEGFKWERVMKFEDGGVVTVTQDSSLQDGE
FIYKVKLRGTNFPSDGPVMQKKTMGWEALSERMYPEDGALKGEVKPRVKLKDGGHYDAE
VKTTYKAKKPVQLPGAYNVNRKLDITSHNEDYTIVEQYERAEGRHSTGGMDELYKAAQRR
GRVGCNDSSDPLVVAASIIGILHLILWILDRL

C – bottom protein band

MVSKGEEDNMAIIKEFMRFKVHMEGSVNGHVFEIEGEGEGRPYEGTQTAKLKVTKGGPLPF
TWDILSPQFMYGSNAYVKHPADIPDYFKLSFPEGFKWERVMKFEDGGVVTVTQDSSLQDGE
FIYKVKLRGTNFPSDGPVMQKKTMGWEALSERMYPEDGALKGEVKPRVKLKDGGHYDAE
VKTTYKAKKPVQLPGAYNVNRKLDITSHNEDYTIVEQYERAEGRHSTGGMDELYKAAQRR
GRVGCNDSSDPLVVAASIIGILHLILWILDRL

8.2.5 Monitoring of background fluorescence in non-transfected cells

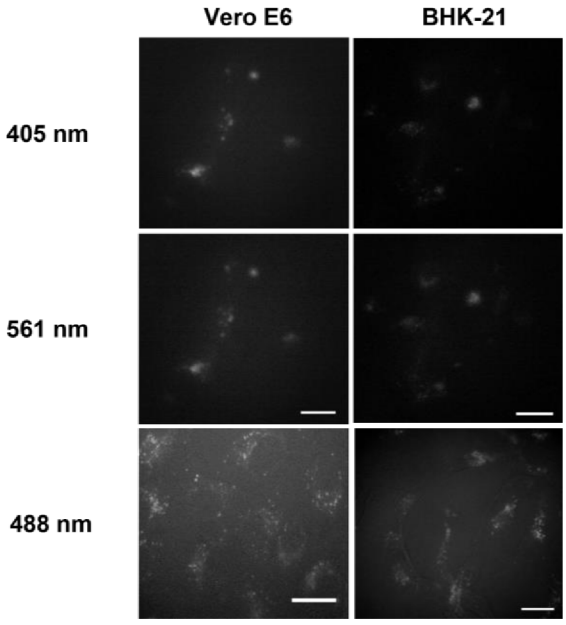

Figure 37 – **Autofluorescence at a given wavelength in both cell types.** Scale bar represents 20 µm.

8.2.6 Monitoring of fluorescence of PAmCherry in living cells, MOI = 1

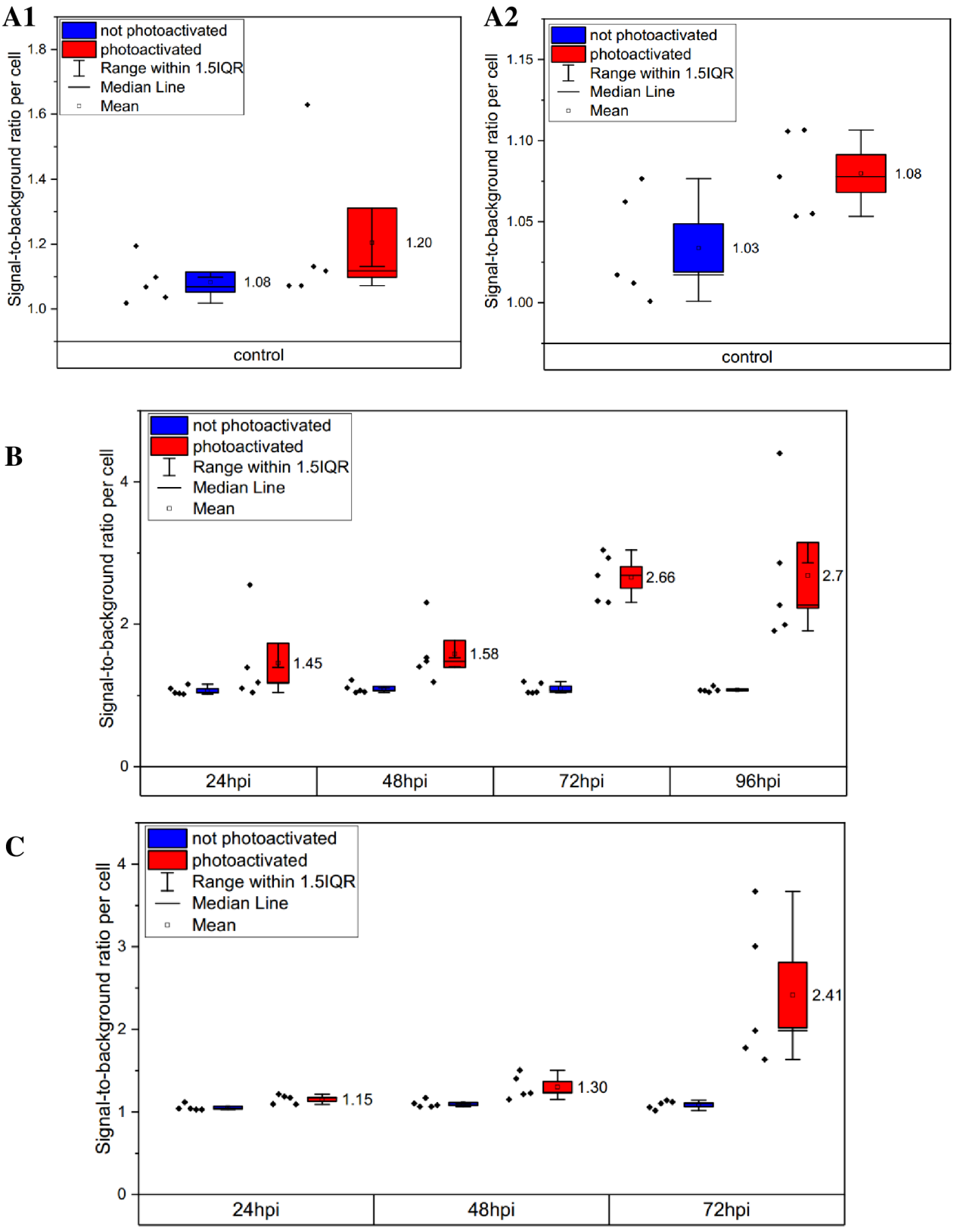

Figure 38 – **Fluorescence intensity analysis of PAmCherry in cells comparing not photoactivated and photoactivated PAmCherry.** A1 – control Vero E6 cells, A2 – control BHK-21 cells, B – Vero E6, MOI = 1, C – BHK-21 cells, MOI = 1, control represents sample cells expressing reporter but without the presence of TBEV.